Development and Dynamics of F-actin in the germ tissue of the telotrophic ovariole of *Rhodnius prolixus*.

Karen Yeow

A Thesis Submitted to
The Faculty of Graduate Studies
In Partial Fulfillment of the Requirements
for the Degree of

MASTER OF SCIENCE

Department of Zoology
Winnipeg, Manitoba

ISBN 0-612-13590-X

Name _____

Dissertation Abstracts International and *Masters Abstracts International* are arranged by broad, general subject categories. Please select the one subject which most nearly describes the content of your dissertation or thesis. Enter the corresponding four-digit code in the spaces provided.

Cell Biology
SUBJECT TERM

0379
SUBJECT CODE

UMI

Subject Categories

THE HUMANITIES AND SOCIAL SCIENCES

COMMUNICATIONS AND THE ARTS
Architecture 0729
Art History 0377
Cinema 0900
Dance 0378
Fine Arts 0357
Information Science 0723
Journalism 0391
Library Science 0399
Mass Communications 0708
Music 0413
Speech Communication 0459
Theater 0465

EDUCATION
General 0515
Administration 0514
Adult and Continuing 0516
Agricultural 0517
Art 0273
Bilingual and Multicultural 0282
Business 0688
Community College 0275
Curriculum and Instruction 0727
Early Childhood 0518
Elementary 0524
Finance 0277
Guidance and Counseling 0519
Health 0680
Higher 0745
History of 0520
Home Economics 0278
Industrial 0521
Language and Literature 0279
Mathematics 0280
Music 0522
Philosophy of 0998
Physical 0523
Psychology 0525
Reading 0535
Religious 0527
Sciences 0714
Secondary 0533
Social Sciences 0534
Sociology of 0340
Special 0529
Teacher Training 0530
Technology 0710
Tests and Measurements 0288
Vocational 0747

LANGUAGE, LITERATURE AND LINGUISTICS
Language
- General 0679
- Ancient 0289
- Linguistics 0290
- Modern 0291

Literature
- General 0401
- Classical 0294
- Comparative 0295
- Medieval 0297
- Modern 0298
- African 0316
- American 0591
- Asian 0305
- Canadian (English) 0352
- Canadian (French) 0355
- English 0593
- Germanic 0311
- Latin American 0312
- Middle Eastern 0315
- Romance 0313
- Slavic and East European 0314

PHILOSOPHY, RELIGION AND THEOLOGY
Philosophy 0422
Religion
- General 0318
- Biblical Studies 0321
- Clergy 0319
- History of 0320
- Philosophy of 0322

Theology 0469

SOCIAL SCIENCES
American Studies 0323
Anthropology
- Archaeology 0324
- Cultural 0326
- Physical 0327

Business Administration
- General 0310
- Accounting 0272
- Banking 0770
- Management 0454
- Marketing 0338

Canadian Studies 0385
Economics
- General 0501
- Agricultural 0503
- Commerce-Business 0505
- Finance 0508
- History 0509
- Labor 0510
- Theory 0511

Folklore 0358
Geography 0366
Gerontology 0351
History
- General 0578
- Ancient 0579
- Medieval 0581
- Modern 0582
- Black 0328
- African 0331
- Asia, Australia and Oceania 0332
- Canadian 0334
- European 0335
- Latin American 0336
- Middle Eastern 0333
- United States 0337

History of Science 0585
Law 0398
Political Science
- General 0615
- International Law and Relations 0616
- Public Administration 0617

Recreation 0814
Social Work 0452
Sociology
- General 0626
- Criminology and Penology 0627
- Demography 0938
- Ethnic and Racial Studies 0631
- Individual and Family Studies 0628
- Industrial and Labor Relations 0629
- Public and Social Welfare 0630
- Social Structure and Development 0700
- Theory and Methods 0344

Transportation 0709
Urban and Regional Planning 0999
Women's Studies 0453

THE SCIENCES AND ENGINEERING

BIOLOGICAL SCIENCES
Agriculture
- General 0473
- Agronomy 0285
- Animal Culture and Nutrition 0475
- Animal Pathology 0476
- Food Science and Technology 0359
- Forestry and Wildlife 0478
- Plant Culture 0479
- Plant Pathology 0480
- Plant Physiology 0817
- Range Management 0777
- Wood Technology 0746

Biology
- General 0306
- Anatomy 0287
- Biostatistics 0308
- Botany 0309
- Cell 0379
- Ecology 0329
- Entomology 0353
- Genetics 0369
- Limnology 0793
- Microbiology 0410
- Molecular 0307
- Neuroscience 0317
- Oceanography 0416
- Physiology 0433
- Radiation 0821
- Veterinary Science 0778
- Zoology 0472

Biophysics
- General 0786
- Medical 0760

EARTH SCIENCES
Biogeochemistry 0425
Geochemistry 0996
Geodesy 0370
Geology 0372
Geophysics 0373
Hydrology 0388
Mineralogy 0411
Paleobotany 0345
Paleoecology 0426
Paleontology 0418
Paleozoology 0985
Palynology 0427
Physical Geography 0368
Physical Oceanography 0415

HEALTH AND ENVIRONMENTAL SCIENCES
Environmental Sciences 0768
Health Sciences
- General 0566
- Audiology 0300
- Chemotherapy 0992
- Dentistry 0567
- Education 0350
- Hospital Management 0769
- Human Development 0758
- Immunology 0982
- Medicine and Surgery 0564
- Mental Health 0347
- Nursing 0569
- Nutrition 0570
- Obstetrics and Gynecology 0380
- Occupational Health and Therapy 0354
- Ophthalmology 0381
- Pathology 0571
- Pharmacology 0419
- Pharmacy 0572
- Physical Therapy 0382
- Public Health 0573
- Radiology 0574
- Recreation 0575
- Speech Pathology 0460
- Toxicology 0383

Home Economics 0386

PHYSICAL SCIENCES
Pure Sciences
Chemistry
- General 0485
- Agricultural 0749
- Analytical 0486
- Biochemistry 0487
- Inorganic 0488
- Nuclear 0738
- Organic 0490
- Pharmaceutical 0491
- Physical 0494
- Polymer 0495
- Radiation 0754

Mathematics 0405
Physics
- General 0605
- Acoustics 0986
- Astronomy and Astrophysics 0606
- Atmospheric Science 0608
- Atomic 0748
- Electronics and Electricity 0607
- Elementary Particles and High Energy 0798
- Fluid and Plasma 0759
- Molecular 0609
- Nuclear 0610
- Optics 0752
- Radiation 0756
- Solid State 0611

Statistics 0463

Applied Sciences
Applied Mechanics 0346
Computer Science 0984
Engineering
- General 0537
- Aerospace 0538
- Agricultural 0539
- Automotive 0540
- Biomedical 0541
- Chemical 0542
- Civil 0543
- Electronics and Electrical 0544
- Heat and Thermodynamics 0348
- Hydraulic 0545
- Industrial 0546
- Marine 0547
- Materials Science 0794
- Mechanical 0548
- Metallurgy 0743
- Mining 0551
- Nuclear 0552
- Packaging 0549
- Petroleum 0765
- Sanitary and Municipal 0554
- System Science 0790

Geotechnology 0428
Operations Research 0796
Plastics Technology 0795
Textile Technology 0994

PSYCHOLOGY
General 0621
Behavioral 0384
Clinical 0622
Developmental 0620
Experimental 0623
Industrial 0624
Personality 0625
Physiological 0989
Psychobiology 0349
Psychometrics 0632
Social 0451

DEVELOPMENT AND DYNAMICS OF F-ACTIN IN THE GERM TISSUE OF THE TELOTROPHIC OVARIOLE OF *Rhodnius prolixus*

BY

KAREN YEOW

A Thesis submitted to the Faculty of Graduate Studies of the University of Manitoba in partial fulfillment of the requirements of the degree of

MASTER OF SCIENCE

I hereby declare that I am the sole author of this thesis.

I authorize the University of Manitoba to lend this thesis to other institutions or individuals for the purpose of scholarly research.

Karen Yeow

I further authorize the University of Manitoba to reproduce this thesis by photocopying or other means, in total or in part, at the request of other institutions or individuals for the purpose of scholarly research.

Karen Yeow

ABSTRACT

The telotrophic ovarioles of *Rhodnius prolixus* contains an extensive F-actin mesh surrounding the trophic core. My research focused on the development of this F-actin mesh during the larval-to-adult ovarian transformation using light and electron microscopy, digital image processing, and immunocytochemistry. F-actin was visualized at the light microscopic level using the F-actin-specific probe, rhodamine-labelled phalloidin, and at the electron microscopic level using immunogold techniques.

The thick and branched F-actin struts characteristic of the adult ovariole form from the F-actin rings of intercellular bridges, or ring canals. These rings form via incomplete cytokinesis of the germ cells. The actin component of the ring canals thickens during development, eventually forming projections that elongate and branch. The actin rings of ring canals act as nucleation sites for the formation of the actin struts. The development of the actin struts occurs in concert with the structural rearrangements that occur during the formation of the membrane-free trophic core region of the tropharium.

The telotrophic ovariole of *Rhodnius* provided an excellent model system in which to study the morphogenesis of a complex, actin-based cytoskeletal structure in intact germ tissue. My results provide the first evidence that ring canals can act as nucleation sites for actin assembly. These results are particularly significant in light of recent findings on the complexity of ring canal development and function in *Drosophila*.

ACKNOWLEDGEMENTS

I would like to thank many people for their advice, support and friendship over the past 4 years.

A thank you to my family for their unconditional support, and to my friends at the Dept. of Zoology for their friendship and discussions, both scientific and otherwise. Special thanks to Gavin Hanke who helped my turtles when they were feeling down, and to Heather Simpson for sharing her snakes. To my lab partners Rene Harrison and Chris Bjornsson, thanks for the bug feeds and making my time at the Huebnerlab so enjoyable. I thank all my Woods Hole friends for their countless emails, and my karate friends for their friendship over the past 4 years. A very special thank you to Randy Tyson for always being there for me.

My thesis committee, Ross McGowan and Mike Sumner, have provided valuable advice and support throughout my research. Thank you also to Lynn Burton for being a wonderful EM technician. Many thanks to Oana Marcu, who provided me with the immunogold protocol that finally worked.

Finally, a sincere thank you to Doc, for the priviledge of working with him. His advice and friendship have meant a lot to me over my undergraduate and graduate years, and I will always treasure the time I have spent as a member of the Huebner lab.

TABLE OF CONTENTS

INTRODUCTION

A fundamental problem in developmental biology is the establishment of germ cell polarity. The development of a multicellular organism from a single egg cell necessitates the existence of a predetermined plan within the oocyte. This information must then be relayed in a specific spatial and temporal pattern in order to generate a normal embryo. In short, the ooplasm harbours a 'latent image' of the embryo. The polarity within the oocyte is later expressed in the major embryonic axes. Thus, the cellular and molecular mechanisms responsible for establishing germ cell polarity organize the basic information necessary for normal embryogenesis to proceed. A complete picture of cellular differentiation and morphogenesis relies upon a knowledge of how germ cells differentiate and maintain their molecular and physiological identities (St. Johnston and Nusslein-Volhardt, 1992).

The cytoskeleton is a key player in the establishment and maintenance of germ cell polarity. Two major components of the cytoskeleton are microtubules and microfilaments. Both the microtubule and the microfilament cytoskeletons play important roles in maintaining the structural polarity in the various compartments of germ tissue. During development, the actin cytoskeleton plays a crucial role in the assembly of a functional oocyte. Many actin-based processes, such as cytokinesis (Robinson et al., 1994), cytoplasmic streaming (Gutzeit, 1986), and nurse cell-oocyte transport (Verheyen and Cooley, 1994) are indispensable for oocyte growth and maturation. Research on the regulation and dynamics of the

actin cytoskeleton has provided significant insights into the mechanisms of establishing germ cell structure and function. Changes in the organization of the actin cytoskeleton regulates the spatial and temporal sequence of events involved in oogenesis (Cooley and Therkauf, 1994). Background information on the biochemistry of actin and actin polymerization, as well as details on the role of the actin cytoskeleton in oogenesis, is provided in Appendix 1.

The Actin Cytoskeleton in Insect Oogenesis

Meroistic ovaries of insects are characterized by the presence of nurse cells, sister cells to the oocytes. The germ cell stem cell, or cystoblast, undergoes a series of incomplete cytokinetic divisions, resulting in the formation of a cellular syncytium. A specific subset of the cell(s) in each syncytium differentiates into the oocyte(s); the rest become nurse cells. Nurse cells play an essential trophic role during oogenesis, synthesizing materials necessary for oocyte growth and maturation. Some of the nurse cell products include organelles like ribosomes, mitochondria, and various RNAs, as well as cytoplasmic determinants crucial for normal embryogenesis, such as the *bicoid* transcript in *Drosophila* (Gottlieb, 1990). Transcription of certain genes (such as *vasa*, *staufen*, *oskar*, and *cyclin B*) occurs in the polyploid nurse cells, and their mRNAs and/or protein products are transported to the oocyte (Lasko, 1992). Thus, the formation of a mature egg and normal embryo depends upon the synthetic activities of the nurse cells as well as a functional transport system to the oocyte.

Drosophila has provided a very successful model that illustrates the role of the actin cytoskeleton in developmental processes. The combination of molecular, biochemical, and cell biological techniques has resulted in a wealth of critical information on the functional role of microfilaments in the establishment of germ cell polarity.

The actin cytoskeleton in the *Drosophila* Polytrophic Ovary

Oogenesis in *Drosophila* is divided into a sequence of stages (King et al., 1982), with the earliest stages occur in the germarium. In region 1 of the germarium, populations of stem cells undergo their initial differentiation into cystoblasts and undergo incomplete cytokinesis to produce the 16-cell cyst (with 15 nurse cells and 1 oocyte). In region 3, the cysts are known as stage 1 egg chambers, ready to enter the vitellarium (Koch and King, 1966). In the vitellarium, progressively more mature egg chambers extend from the anterior to the posterior of the ovariole. The egg chambers have been divided into stages 2 to 14, where the stage 14 oocyte is ready for fertilization.

Bulk nurse cell cytoplasmic transport to the oocyte can be visualized during the later stages of vitellogenesis (Gutzeit and Koppa, 1982). By stage 10, the oocyte makes up half the volume of the egg chamber. The rapid phase of cytoplasmic transport to the oocyte occurs in Stage 11, resulting in a doubling of the oocyte volume in about 30 minutes, along with regression of the nurse cell cluster (Gutzeit, 1986; Xue and Cooley, 1993). The nurse cell nuclei remnants

(including nuclear membranes and chromatin) are excluded from the flow of cytoplasm through the cytoplasmic bridges.

There are three distinct subpopulations of actin filaments in the *Drosophila* egg chamber: the subcortical actin network in the nurse cells and oocyte, the cytoplasmic actin bundles that appear during the rapid phase of cytoplasmic transport, and the F-actin rings associated with cytoplasmic bridges. However, it is difficult to isolate the changes occuring in the actin cytoskeleton from the changes resulting from germ cell development. Since the development of specialized cytoskeletal structures occurs in concert with such fundamental processes as cytokinesis and intercellular transport, actin and its associated proteins are part of a complex interacting system whose main function is to support normal development.

Microfilaments (along with microtubules) play an important role in cytoplasmic transport to the oocyte (Therkauf et al., 1992; Cooley and Therkauf, 1994). Just before the onset of rapid cytoplasm transport, major rearrangements in the actin cytoskeleton occurs in stage 10 egg chambers. An extensive series of cytoplasmic actin bundles appears in the nurse cells, forming cables that extend from the nuclear membrane to the plasma membrane. The pattern of actin staining in nurse cells of late stage 10 egg chambers resembles spokes on a wheel. The cytoplasmic actin bundles anchor nurse cell nuclei in place, allowing large amounts of nurse cell cytoplasm to be transported freely to the oocyte. While the nuclei are anchored in place, the subcortical actin network in the nurse cells contracts,

expelling nurse cell cytoplasm into the oocytes. Rhodamine-labelled phalloidin staining reveals a distinct subcortical actin network associated with the nurse cell membranes. Examination of the subcortical actin networks indicates that they are responsible for generating the contractile force that squeezes cytoplasm into the oocyte (Gutzeit, 1986).

A variety of actin-associated proteins are involved in the formation of the cytoplasmic actin bundles. *Chickadee* (encoding a *Drosophila* homolog of profilin), *singed* (encoding a fascin-like protein) and *quail* (encoding a villin-like protein) are three mutants that fail to develop these actin bundles, resulting in the production of small, infertile eggs. In the absence of the cytoplasmic actin bundles, nurse cell nuclei become lodged in the ring canals during the final phase of cytoplasmic transport, blocking the passageway for further transport of material to the oocyte.

Development and Function of Ring Canals in the Polytrophic Ovary

In addition to the subcortical and cytoplasmic actin networks, the F-actin rims of rings canals constitute another important component of the actin cytoskeleton. Ring canals are formed by modifying the usual process of cytokinesis (Satterwhite and Pollard, 1992). Electron microscopy reveals a bridge connecting the cytoplasm of adjacent cells. The bridge consists of an electron-dense rim, resembling a bracket in cross-section (Robinson et al., 1994). When they are first formed in the germarium, they measure approximately 1 μm in diameter. In the mature egg chamber, the bridges increase in size to 7-10 μm,

enabling the passage of mitochondria, ribosomes, endoplasmic reticulum and other organelles (Warn et al., 1985). A highly vesiculated structure, known as the fusome, extends throughout the cytoplasmic bridges, possibly functioning to stabilize the cleavage furrow until the ring canals are established (King and Storto, 1988, Lin et al., 1994). Ring canals are finally lost following nurse cell breakdown after the rapid cytoplasmic transport phase (Cooley et al., 1992).

Cleavage furrow arrest and ring canal development are not well understood. *hu-li tai shao* and *kelch* are female-sterile mutations that either disrupt ring canal structure or cytoplasmic transport through the ring canals. *Drosophila* females bearing mutations at the *hu-li tai shao* (*hts*) locus produce egg chambers with less than 15 nurse cells and in most cases, lacked an oocyte (Yue and Spradling, 1992). In addition, the cytoplasmic bridges appeared abnormal, lacking the F-actin rings. Immunofluorescence studies reveal that hts localizes to the inner rim of ring canals, along with F-actin. In wild-type egg chambers, these 2 proteins form a compact inner rim in the ring canals (Robinson et al., 1994). The *hts* cDNA sequence encodes a homolog of adducin. The effects of the *hts* mutations on ring canals can be explained by lack of the actin-binding activity of adducin. The *hts* protein may be needed to assemble normal ring canals. In the absence of a functional ring canal, intercellular communication between the dividing germline cells may be impaired, resulting in an abnormal number of nurse cells.

Kelch mutants are defective in cytoplasmic transport from the nurse cells to the oocyte. Like hts, the *kelch* protein localizes specifically to ring canals. Unlike

hts, kelch does not appear to be required for initial ring canal formation. However, in later stage *kelch* egg chambers, the actin and hts in the ring canals extend into the lumen of the cytoplasmic bridge, instead of forming a compact rim. This suggests that kelch interacts with actin and hts to form the highly organized inner ring canal rim (Xue and Cooley, 1993).

Ring canal maturation involves the sequential addition of proteins as the egg chamber matures within the germarium (Robinson et al., 1994). At least one phosphotyrosine protein can be detected on the ring canals of newly-forming egg chambers in region 1 of the germarium. The role of phosphotyrosine protein(s) in the ring canal remains unknown. Hts and actin are present in region 2a, shortly after mitotic divisions are complete. Kelch is the last protein to be recruited to the ring canals. In the later stages of oogenesis, the ring canal rim is compacted, and all four of these proteins are co-localized. It is not clear whether more proteins are added to the ring canal as it matures from stage 3 to stage 10.

Studies on *Drosophila* mutants have provided valuable information on the molecular composition and development of ring canals. Despite this, little is known about the function of ring canals in the polytrophic ovary. It is currently speculated that fine microfilament "tracks" exist in the lumen of intercellular bridges, facilitating transport of specific molecules through the ring canals (Bohrmann and Biber, 1994). However, such microfilament pathways have yet to be resolved. Given the complexity of their molecular composition, and their highly organized development, it is likely that ring canals play a complex regulatory role in germline

communication.

The Actin Cytoskeleton in the Telotrophic Ovary

Telotrophic ovaries have a dramatic exaggerated structural and functional polarity in comparison to polytrophic ovaries. Telotrophic ovaries are found in the Polyphage Coleoptera, Megaloptera, and Hemiptera (Huebner, 1982). The telotrophic ovarioles of the hemipteran *Rhodnius prolixus* provide an excellent model system in which to study cytoskeletal function in germ tissue. The seven ovarioles which comprise the ovary are covered by double ovariole sheaths (reviewed in Huebner, 1982). Beneath the sheaths is the basal lamina, enclosing the germ cells and associated follicle cells. Each adult ovariole is composed of a tropharium, a complex syncytium of nurse cell compartments that is cytoplasmically connected to the growing oocytes by elongated intercellular bridges known as trophic cords. A small population of mitotic germ cell stem cells resides at the anterior tip of the tropharium. The syncytial arrangement of nurse cells with the nurse cell lobes opening into a central, membrane-free zone known as the trophic core. The tropharium is normally covered by inner sheath cells that lie in between the nurse cell lobes and basement membrane. Tracer microinjection studies verify that the nurse cell lobes connect to the oocytes via the central trophic core and cords (Huebner, 1982). In contrast to the *Drosophila* ovariole, in which egg chambers are found in sequential development (like beads on a string), all of the nurse cells in the *Rhodnius* ovariole are contained within the tropharium, which in

turn is connected to a series of growing oocytes.

Research Problem: The trophic core F-actin mesh in the *Rhodnius* ovariole

The cytoarchitecture and rich endowment of cytoskeletal components of the *Rhodnius* ovariole render it ideal for studying the role of cytoskeletal elements in polarized cytoplasmic transport and the establishment of cell polarity. Much background work has been done on the cell biology of the *Rhodnius* telotrophic ovary. Studies so far have mainly focused on the microtubule cytoskeleton (Valdimarsson and Huebner, 1989; Harrison and Huebner, 1994). However, McPherson and Huebner (1993) have analysed the actin cortical cytoskeleton in the oocyte.

Huebner and Gutzeit (1986) discovered that the adult *Rhodnius* tropharium has an elaborate F-actin mesh surrounding the trophic core. Little is known about the development of this structure, its function, and the general picture of actin in nurse cells of telotrophic ovarioles. Fluorescent staining with rhodamine-labelled phalloidin revealed that the interconnecting network of microfilaments encases the microtubule-rich core. The actin filaments in the core are organized in an anisotropic mesh, rather than in parallel arrays. The entire structure is highly stable in detergent extraction procedures, suggesting that the actin filaments are highly cross-linked (Huebner and Gutzeit, 1986). Some of these actin struts branch out into the nurse cell lobes. Posteriorly, the actin network ends at the nurse cell-prefollicular interface. Although initially it was thought that actin bundles were

absent from the trophic cords, subsequent analysis of the cords revealed the presence of actin struts extending into the cortex of the cords (McPherson and Huebner, 1993).

The trophic core F-actin mesh has also been found in several other hemipteran insects with telotrophic ovarioles (Gutzeit and Huebner, 1986). Rhodamine-labelled phalloidin staining of the ovaries from these species reveals a characteristic microfilament network surrounding the trophic core. In species with polytrophic ovaries, as well as non-hemipterans with telotrophic ovaries, no such pattern of microfilaments was observed. Instead, the nurse cell membranes were associated with a subcortical F-actin network.

Despite the discovery of the telotrophic F-actin mesh, we know little of its development, function or composition. The objective of my research is to elucidate the sequence of developmental events in the formation of the trophic core F-actin mesh. Such information is important for several reasons. Little is known about the mechanisms of actin polymerization in general. Analysis of the developmental events can shed light on the mechanisms involved in actin nucleation and assembly. Secondly, based on evidence in *Drosophila*, actin microfilaments likely play important roles in the fundamental cellular processes involved in generating the complex telotrophic syncytium. The void of information on the development of the trophic core must be addressed before its function can be fully explored further. The enhanced abundance of actin, and the exaggerated syncytial structure and polarity of the telotrophic ovariole compared to *Drosophila* ovarioles indicate

that an examination of actin in the telotrophic system may lead to insights on ring canal and actin morphology not easily accessible in the polytrophic ovary.

There are 5 larval instars in the *Rhodnius* life cycle before the adult. The major differentiation step that involves transformation from a larval ovariole to the polarized adult ovariole occurs in the 5th, or penultimate, instar. During the 5th instar, a complex series of growth, differentiation, and restructuring events transforms the larval ovary into a functional adult ovary. Development from one stage to the next is triggered by a blood meal. The time of feeding can therefore be used as an indicator of the stage of development within a particular instar. Development of the larval ovary involves germ cell mitosis and proliferation throughout the first four larval instars (Huebner, 1984). The larval-adult ovarian transformation occurs over a period of approximately 24 days after a blood meal in the 5th, or final, instar.

The 5th instar ovary is much smaller in size in comparison to the adult ovary, and is sparsely tracheated. Developmental events in the larval-adult ovarian transformation are divided into three phases: proliferative (unfed - 8 DPF), early differentiation (9 - 15 DPF), and late differentiation (16 DPF - moult) (Lutz, 1979). In the undifferentiated larval ovary, the germ cells are housed in a unit known as the germarium. The unfed ovariole contains germ cells surrounding a central trophic core area. The undifferentiated germ cells undergo mitotic divisions, and increase in size, thereby enlarging the germarium.

The early differentiation phase is marked by the beginning of regional

specialization within the germarium compartments. Midway through this stage, nurse cell and oocyte compartments are distinguishable. Developing oocytes are marked by a less intense staining of the cytoplasm, the lack of a distinct nucleolus, and the presence of synaptonemal complexes. The germ cells at the apical portion of the germarium begin to differentiate into nurse cells.

In the late differentiation phase, morphology of the germarium begins to resemble that of the adult. The nurse cells at the base of the germarium become increasingly basophilic, and groups of nuclei are present within a common cytoplasm. Membrane fusions in the central region of the germarium occur, resulting in a defined trophic core region. Prefollicular cells migrate into the region of developing oocytes, and the trophic cords connecting the oocytes to the trophic core become discernible (Lutz and Huebner, 1981).

As in the polytrophic ovariole, the nurse cell-oocyte syncytium arises via incomplete cytokinetic divisions of germ cell stem cells (Lutz and Huebner, 1981). Intercellular bridges have been reported in the fifth instar germarium (Huebner and Anderson, 1972), suggesting that complex restructuring and cellular fusions must occur in the transformation to the adult ovarian structure. Nurse cell compartments associate with one another in two ways: through intercellular bridges from incomplete cytokinesis, and by membrane fusions resulting in groups of active nurse cell nuclei occupying a common cytoplasm (Lutz and Huebner, 1981). The earliest oocytes associate with the other germ cell compartments, including other oocytes, only via intercellular bridges. Interconnecting bridge systems provide a

direct route for transport of material from the nurse cells to the oocytes via the trophic core and cords.

A central, nuclei-free trophic core is present throughout the fifth instar, but undergoes massive membrane restructuring during the late differentiation phase (Lutz and Huebner, 1981). In the proliferative and early differentiation phases, the core consists of a complex intertwined array of cell processes (Huebner and Anderson, 1972). Most germ cells are in cytoplasmic continuity with the core, and profiles of intercellular bridges are visible within the core (Lutz and Huebner, 1981). The lateral densities of intercellular bridges are visible within the core. During the restructuring of the core, membrane fusions and cellular reorganization form a central, membrane-free zone in the germarium. Membrane fusions also occur in the basally located nurse cell compartments. These multinuclear groups remain connected to other groups of nuclei through intercellular bridges (Lutz and Huebner, 1981).

As shown in this thesis, the F-actin mesh develops in concert with these complex cytoarchitectural rearrangements occuring in the tropharium. In order to describe the formation of the F-actin mesh in the trophic core, various techniques were used to accurately depict the organization of the F-actin-based cellular structures at various developmental stages. Rhodamine-labelled phalloidin, a specific F-actin stain, and transmission electron microscopy (TEM) provided a good overview of the organization and formation of the F-actin network. Immunoelectron microscopy provided additional evidence that the fibrous struts seen in TEM were

composed of actin. Digital deconvolution of fluorescence light microscopic images enabled the resolution of fine detail in the actin-based structures.

Rhodamine-labelled phalloidin staining and TEM demonstrate that the F-actin mesh arises initially from membrane-associated F-actin, in particular, the F-actin rings of intercellular bridges. The F-actin rings thicken, and gradually form projections that elongate and branch. Studies on intercellular bridges in *Drosophila* have indicated that their molecular composition and development are far more complex than previously thought. It is therefore significant that the ring canals in the telotrophic ovary play a role in the formation of such an elaborate cytoskeletal structure. In *Rhodnius*, the F-actin rings of intercellular bridges presumably are the nucleation sites for the formation of actin struts. During the transformation of the trophic core from its larval to adult condition, the actin rings of intercellular bridges somehow dissociate from their adjoining membranes, thicken, and form fibrous struts that elongate and interconnect. These results are especially significant as this is the first report of intercellular bridges giving rise to a complex cytoskeletal structure.

The location of the trophic core actin mesh, coupled with its highly stable nature (Huebner and Gutzeit, 1986), suggests that it may function mechanically in the organization of the tropharium and its core. The thick actin struts may physically separate the nurse cell lobes from the microtubule-rich trophic core, thereby maintaining the major transport pathway from the tropharium to the core and in turn, eventually to the oocytes.

MATERIALS AND METHODS

Animal Material

A culture of *Rhodnius prolixus* is maintained year-round in a Controlled Environments Inc. incubator at 26°C and 70% relative humidity. The insects are contained in 500 ml glass jars with wire mesh lids. Within each jar, two pieces of fluted filter paper are used for urine absorption and as a substrate for egg deposition. The animals were fed upon shaven bellies of rabbits once every 2-4 weeks. Experimental animals were fed as required.

Staging of Ovarioles

Unfed, newly molted fifth instars were selected for experiments. Previous studies on the *Rhodnius* larval-adult ovarian transformation have used the time of feeding of the 5th instar as a reference point for staging ovarian development (Lutz and Huebner, 1980; 1981). These studies reported that fifth instarts molted into adults 21 days post feed (dpf). In my study, I have found that the pattern of feeding and molting varied within different batches of animals fed at the same time, as well as within the same batch. However, the average time from feeding to adult molt was 24-26 dpf. Despite a certain degree of variability, days post feed provided a suitable indicator of developmental stage.

Dissection Techniques

All dissections were performed using Wild M3 or M5 dissecting

microscopes. Insects were dissected in Sylgard® or dental wax-lined petri dishes under saline (*Rhodnius* ringers [modified after O'Donnell, 1985,] (129 mM NaCl, 8.6 mM KCl, 2.0 mM $CaCl_2$, 8.5 mM $MgCl_2$, 15 mM Bis-Tris and 34 mM glucose, pH 6.9-7.0). The dorsal cuticle was removed, and the ovarioles transferred to a separate petri dish containing fresh saline. Tracheoles and ovarian sheaths were removed and the ovarioles separated. For transmission electron microscopy (TEM) the ovarioles were not dissected further. Some of the ovarioles were desheathed for fluorescence and immunofluorescence observations.

Fluorescence Microscopy

Live ovarioles were permeabilized for 5 mins in 0.1% Triton X-100 in microfilament (MF) buffer (80 mM KCl, 20 mM PIPES, 5.6 mM glucose, 1.5 mM $MgCl_2$, 1.5 mM $CaCl_2$, and 10 mM EGTA, at pH 7.1-7.2). The ovarioles were then washed with at least 3 changes of MF buffer for 10-15 mins, and transferred into fixative. The fixative consisted of 3-4% paraformaldehyde in MF buffer (pH 7.2-7.2). Ovarioles were gently swirled around in the fixative, and allowed to fix for 15 mins. Subsequently, they were washed with at least 4 changes of MF buffer over a minimum of 20 mins. Ovarioles in a drop of MF buffer were stained by adding an equal amount of buffer containing 10 µg/ml rhodamine-labelled phalloidin so the final concentration was 5 µg/ml. The slide was covered with a vaseline-edged coverslip to minimize evaporation, and placed in a petri dish lined with moist filter paper.Staining was performed in the dark at room temperature (approximately

24°C), for 20-30 mins. After staining, the ovarioles were washed in MF buffer for a minimum of 45 mins, using at least 6 changes of wash medium. All the above steps were performed at room temperature (24°C). The ovarioles were mounted in PBS with 1-5 mg/ml n-propyl gallate dissolved in it to minimize photobleaching. Preparations were viewed with a Zeiss Photo II epifluorescence microscope, using the filter set for rhodamine. Images were captured directly onto Kodak T-Max 100 film using a Zeiss Photo II camera. The film was processed routinely using Kodak T-Max developer.

Image Processing

Rhodamine-labelled phalloidin stained ovarioles were viewed with a Zeiss Photo II epifluorescence microscope using the filter set for rhodamine. Images were captured using a Dage 66 SIT camera and processed using the Image-1 (®Universal Imaging) image processing system in a 486 PC computer. To obtain clearer fuorescence images of the in focus plane and minimize the background fluorescence from the out of focus plane deconvolution routines in Image-1 were run. A deconvolution journal which executed a sequence of functions that subtracted the averaged above and below focus fluorescence images and subtracted the result from the focal plane of interest yielded images which revealed details obscured in normal fluorescence images. Images were stored on Bernoulli disks. Negatives of deconvolution images were obtained using a Polaroid freeze-frame equiped with a 35 mm camera. Stored images were displayed and captured

on T-Max 100 film in the freeze-frame camera.

Transmission Electron Microscopy

Ovarioles were dissected out in sterile *Rhodnius* Ringers, detracheated, and separated. They were then transferred directly into fixative. The fixative used was a modified Karnovsky's fixative consisting of 3% glutaraldehyde, 1% paraformaldehyde, and 0.05% $CaCl_2$ 0.1M sodium cacodylate buffer, pH 7.2-7.4. The tissue was fixed for 1-1.5 hours at 4°C, then washed in 0.1M sodium cacodylate buffer, pH 7.2, at 4°C for 1 hour. Postfixation was carried out at 4°C, using 1% OsO_4 in 0.1M sodium cacodylate buffer for 30 mins. Following postfixation, the ovarioles were given a brief wash in 0.1M sodium cacodylate buffer, and dehydrated in a cold (-20°C) series of graded ethanol concentrations (70%, 80%, 95%, and absolute ethanol). Once in 100% alcohol, the tissue was allowed to warm to room temperature, and four subsequent changes of absolute ethanol were done at 30 min intervals. The final ethanol change was replaced with a 1:1 mixture of ethanol and acetone for 15 mins. This step was followed by 2 consecutive changes of pure acetone, for 15 mins each. The ovarioles were then allowed to infiltrate overnight in a 1:1 mixture of acetone and Epon-Araldite embedding medium (2.5 parts Epon 812, 2 parts Araldite 502, 6 parts DDSA, with 3% DMP-30 as catalyst). The next day, the tissue was transferred into fresh embedding medium and allowed to infiltrate for 4-5 hours. Individual ovarioles were separated using minutin pins, and embedded in fresh embedding medium. The

blocks were allowed to polymerize for at least 24 hours at 55-60°C.

Silver-gold sections were cut with a Sorvall Porter Blum MT2B ultramicrotome. Sections were collected on naked 200 hex copper grids. Grids were stained in alcoholic uranyl acetate for 20-30 mins, washed in distilled water, and stained in lead citrate for 2 mins (modified Venable and Coggeshall, 1965). Grids were examined in a Hitachi H7000 scanning transmission electron microscope, using the transmission electron microscope function, at an accelerating voltage of 75 kV. EM negatives were taken on Kodak electron microscopic film 4489, and developed routinely using Kodak D19 developer.

Immunoelectron Microscopy

Freshly-removed ovarioles were fixed in 2% glutaraldehyde and 1% paraformaldehyde in MF buffer at pH 7.2 - 7.3 for 1 hour at room temperature. The tissue was then thoroughly washed in several changes of MF buffer over a 30 min period, and dehydrated in several changes of 70% ethanol for 30 mins. This was followed by dehydration in pure ethanol for 30 mins - 1 hour. The ovarioles were then infiltrated in a 1:1 mixture of pure ethanol and LR White over 1 hour. Infiltration was completed by a final infiltration of the tissue into pure LR White solution, for 1 hour. The latter 2 steps were performed on a rocker to ensure maximum infiltration. Individual ovarioles were separated and embedded in gelatin capsules, filled fully and tightly capped. Polymerization was carried out in a vacuum oven, for 24 - 28 hours, between 55 - 60°C.

Silver-gold sections were cut on a Sorvall Porter-Blum MT2B microtome, and collected on 400 mesh nickel grids. The sections were etched for 5 mins in a 5% solution of H_2O_2 in distilled water. They were then washed briefly in PBS, and blocked in 3% BSA in PBS for 1 hour. Following a brief rinse in PBS they were incubated in a 1:40 dilution of anti-chicken gizzard actin antibody (Sigma A-2668). The 1° antibody was diluted in 3% BSA in PBS. This was followed by a 30 - 45 min wash in PBS, and incubation in 10 nm colloidal gold-conjugated goat anti-rabbit (Sigma G-3779) (1:60 dilution in 3% BSA in PBS), for 1 hour. The grids were then washed with several changes of PBS for 45 mins-1 hour, rinsed in distilled water, and allowed to air dry.

Grids were stained for 15-20 mins in saturated aqueous uranyl acetate, and 30 sec. in lead citrate (see the TEM section). The grids were viewed at 75 kV. In order to minimize sections collapsing under the electron beam, the sections were allowed to "warm up" for 30 secs-1 min under low magnification with a low brightness setting. The brightness setting was increased very slowly to the optimal level for viewing before increasing the magnification.

Photography Techniques

Light and electron micrograph negatives were printed on Ilford Rapid Multigrade III RC polycontrast glossy paper, using a #4 polycontrast filter. The freeze-frame negatives of the deconvolution images were printed using the #5 polycontrast filter. The prints were processed in an Agfa print processor using Ilford

activator and stabilizer, and made permanent by fixation in Edwal's paper fixative, made up according to the manufacturer's instructions. The prints were then washed for 20-30 mins, and left to air-dry at room temperature.

RESULTS

General Features of the F-actin mesh in the *Rhodnius* ovariole

The *Rhodnius* ovariole is divided into two components: the tropharium, which houses the nurse cells, and the vitellarium, containing the developing oocytes and follicle cells. The nurse cells are connected to the oocytes via the trophic core and cords. The tropharium consists of a syncytial arrangement of nurse cells, whose lobes open into the central, membrane-free trophic core (Diagram 1b).

The F-actin mesh in the adult is found in the trophic core (Huebner and Gutzeit, 1986), and extends into the trophic cords (McPherson and Huebner, 1993). The actin struts form a complex network that encircles the trophic core (Diagram 1b). In the early 5th instar ovariole, no actin struts are present (Diagram 1a). The larval ovariole consists of undifferentiated germ cells housed in the germarium. In the early stages of 5th instar development, the F-actin rims of intercellular bridges and general membrane-associated F-actin are the only distinct F-actin structures within the germarium. The following results cover the development of the complex adult F-actin structure from the earliest 5th instar stages.

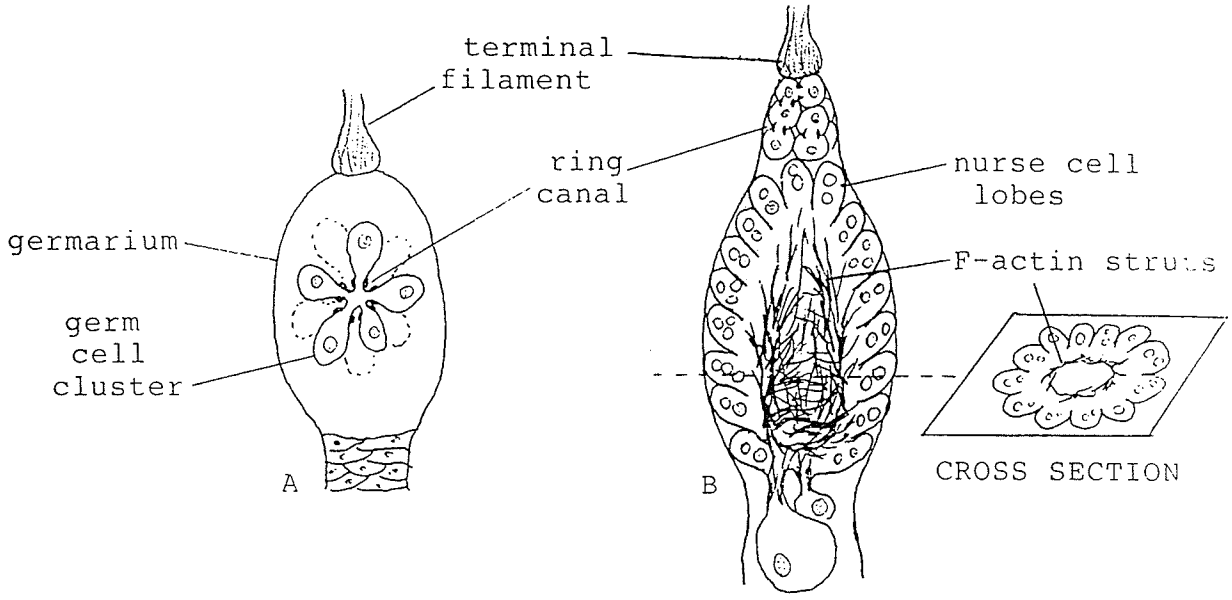

Diagram 1. Actin distribution in the 5th instar and adult ovarioles.
a).The 5th instar ovary consists of individual sibling cell clusters which fuse during the larval-adult ovarian transformation to create the syncytium seen in the adult. The F-actin rims of intercellular bridges give rise to the F-actin mesh surrounding the adult trophic core.
b). The adult ovariole, showing the location of the F-actin mesh. The actin mesh in the adult encircles the trophic core, forming a hollow, anisotropic cylinder (see cross-section).

Early Proliferative Stages (0-10 dpf)

In the earliest stages of development, rhodamine-labelled phalloidin staining reveals a general pattern of background actin staining, due to membrane-associated F-actin (Plate 1). The muscle-rich terminal filament labels strongly, in contrast to the germarium (Figs. 1, 2). The prefollicular area of somatic cells rich in F-actin stain more intensely than the germarium (Figs. 1,2). There is no evidence of actin struts in the developing germarium (Fig. 3).

F-actin highlighting the ring canals is not clearly visible in the germarium until at least 4-6 dpf (compare Figs. 4, 5, 8). Ring canals seen with rhodamine-

labelled phalloidin appear as distinct oval-shaped profiles within the mass of germ tissue (Figs. 5, 8). Even with fluorescence microscopy the F-actin stained rings cannot be seen sharply, due to the general fluorescence of the focal planes above and below each particular ring canal. However, digital image deconvolution of conventional fluorescence images enables the circular fluorescent profiles to be resolved as rings (Figs. 31, 32). Digital deconvolution greatly improves the clarity of the in-focus plane by removing much of the signal from the out-of-focus planes.

TEM of ring canals in early stage ovarioles reveals that the ring canals connect adjacent cells in the germarium. These bridges are easily recognized by their distinctive electron-dense membrane morphology (Figs. 6, 7, 9, 12, 13). A cross-section through a bridge illustrates the electron-dense, bracket-shaped membranous area and the central cytoplasmic continuity connecting adjacent cells (Figs. 12, 13). In the early stages of incomplete cytokinesis, the mid-body is still present in the cytoplasmic bridges connecting adjacent cells (Lutz, 1979). Fig. 9 depicts an intercellular bridge with the midbody and remnants of the spindle microtubules still visible. The membranous portion of the bridges contain an electron-dense material (Fig. 9), some of which is presumably the F-actin seen in fluorescence microscopy (Fig. 7)

As the developing ovariole increases in size during the proliferative phase (5-8 dpf), the population of germ cells increases in number by incomplete cytokinesis, which reflects the increasing number of ring canals. Within the germarium (Figs. 10, 11), ring canals often occur in clusters, with 3-5 ring canals

in close proximity (Figs. 11, 12, 13). There is still no sign of distinct F-actin struts in the germarium. The general level of background F-actin staining in the germ cells increases with the increasing size and complexity of the germarium (Figs. 10, 11).

Early Differentiation Phase (10-16 dpf)

The ring canals become even more prevalent and appear more prominent as development progresses. The germarium continues to increase in size and complexity, as membrane fusions and restructuring continues to occur in the larval trophic core area. The amount of background F-actin staining continues to increase in comparison to the early proliferative stage. Towards the anterior of the germarium, the F-actin rings of intercellular bridges appear thinner than those in the posterior region of the germarium (Figs. 14, 15, 17, 18). The ring canals in the posterior region label strongly with rhodamine-labelled phalloidin, despite the strong background signal from the out-of-focus tissue. The detail in individual ring canals are obscured by the out-of-focus plane fluorescence, an inevitable problem in conventional fluorescence microscopy of whole mounts. However, digital deconvolution minimizes this problem and reveals that the circular F-actin profiles are donut-shaped rings of F-actin (Figs. 33, 34).

Now, the core area of the germarium consists of an elaborate arrangement of membranes and cellular processes, along with mitochondria, Golgi complexes, ribosomes, and breakdown elements such as lamellar bodies and multivesicular

bodies (Lutz, 1979). As the trophic core area continues to develop, many intercellular bridge profiles are visible within the core (Figs. 19, 21, 22). Cross-sections of ring canals at this stage illustrates the increase in electron-dense material at the rims of the ring canals (Fig. 20). Ring canals in the trophic core area are frequently associated with a complex organization of cell membranes (Fig. 22). The result is thickened dense deposits at the bridge and extending to the adjacent cell membrane areas (Figs. 21, 22).

By approximately 13-15 dpf, the circular F-actin profiles are more numerous and prominent (Figs. 27, 28). Now, short fibrous actin struts appear in the germarium (Figs. 27, 28). The deconvolution images at this stage (Figs. 33, 34) illustrate that many of the bright fluorescent, circular structures are the circular profiles of ring canals seen in the earlier stages, only with thicker rims (Figs. 31, 32). TEM depicts the fibrous actin structures in cross section (Figs. 23-26). These structures are more pronounced in the basal area of the tropharium, in the developing trophic core (Fig. 18). Throughout the early differentiation phase, longitudinal sections of ring canals illustrates their gradual thickening, eventually forming the fibrous, circular structures visible in the posterior half of the ovariole (Figs. 23-26).

Late Differentiation Phase (16 dpf - molt)

The late differentiation phase is marked by a further increase in the number of fibrous, circular actin structures. The F-actin rims of intercellular bridges begin

to transform into a variety of irregular, but basically circular, shapes (Figs. 37, 41, 42). Actin struts in the posterior region of the germarium now elongate, thicken, and branch (Figs. 38, 39, 41, 42). The membranes reorganize and disappear in the restructuring of the tropharium. Many of the membrane fusions and rearrangements continue in the trophic core, creating a central, membrane-free zone. The F-actin structures within the core area are no longer membrane-associated (Figs. 37, 40, 41, 42). Just before molt, the interconnecting actin network that will eventually encircle the trophic core in the adult begins to form as the actin struts become more complex and interconnected (Figs. 43, 44). A distinct banding pattern is visible in some of the thick F-actin fiber in the adult (Figs. 35, 36, 48). TEM reveals numerous branched, fibrous actin struts in the trophic core area (Fig. 45). Digital deconvolution highlights the in-focus fluorescence image of the F-actin struts (Figs. 35, 36). Some of the thickened circular ring canal profiles and the banding pattern in the branched fibers are more clearly seen, even at the light microscopic level.

After the molt to the adult, the actin mesh completes its final maturation. At the anterior portion of the germarium, actin morphogenesis continues with the ring canals continuing to thicken, and elongating actin struts eventually linking up those in the posterior region (Figs. 48, 49). Immunocytochemistry using immunogold techniques indicates that the long, fibrous structures seen in the membrane-free trophic core (Fig. 45) consist of F-actin (Figs. 46, 47). The adult F-actin mesh completes development approximately 6-8 days after the adult molt.

Attempts to localize other ring canal-associated proteins found in *Drosophila* using immunofluorescence techniques and antibodies to *Drosophila* proteins have been unsuccessful thus far. Details and preliminary results obtained are provided in Appendix II.

Plate 1

Actin distribution in the early 5th instar ovariole: early proliferative stage

Figs. 1 & 2.
Rhodamine-labelled phalloidin staining of whole mounts of 5th instar ovarioles (1 and 3 dpf, respectively). The terminal filaments (T) fluoresce brightly. There is also positive staining of the prefollicular area (P). Only a general pattern of F-actin staining in the germ tissue (G) is seen in these early stages.
800X; 1,250X

Fig. 3.
This higher magnification view of a 1 dpf germarium shows the cell membrane-associated Factin staining of the germ cells (arrows).
2,000X

Fig. 4.
At 3 dpf, the circular profiles of ring canals are visible within the germarium (arrows). Due to the size and thickness of the whole mount, the ring canals cannot be seen any clearer without confocal microscopy.
2,100X

Fig. 5.
TEM of the larval trophic core demonstrates that there are no distinct fibrous structures in this region of the germarium. Membrane processes and microtubules are seen.
15,000X

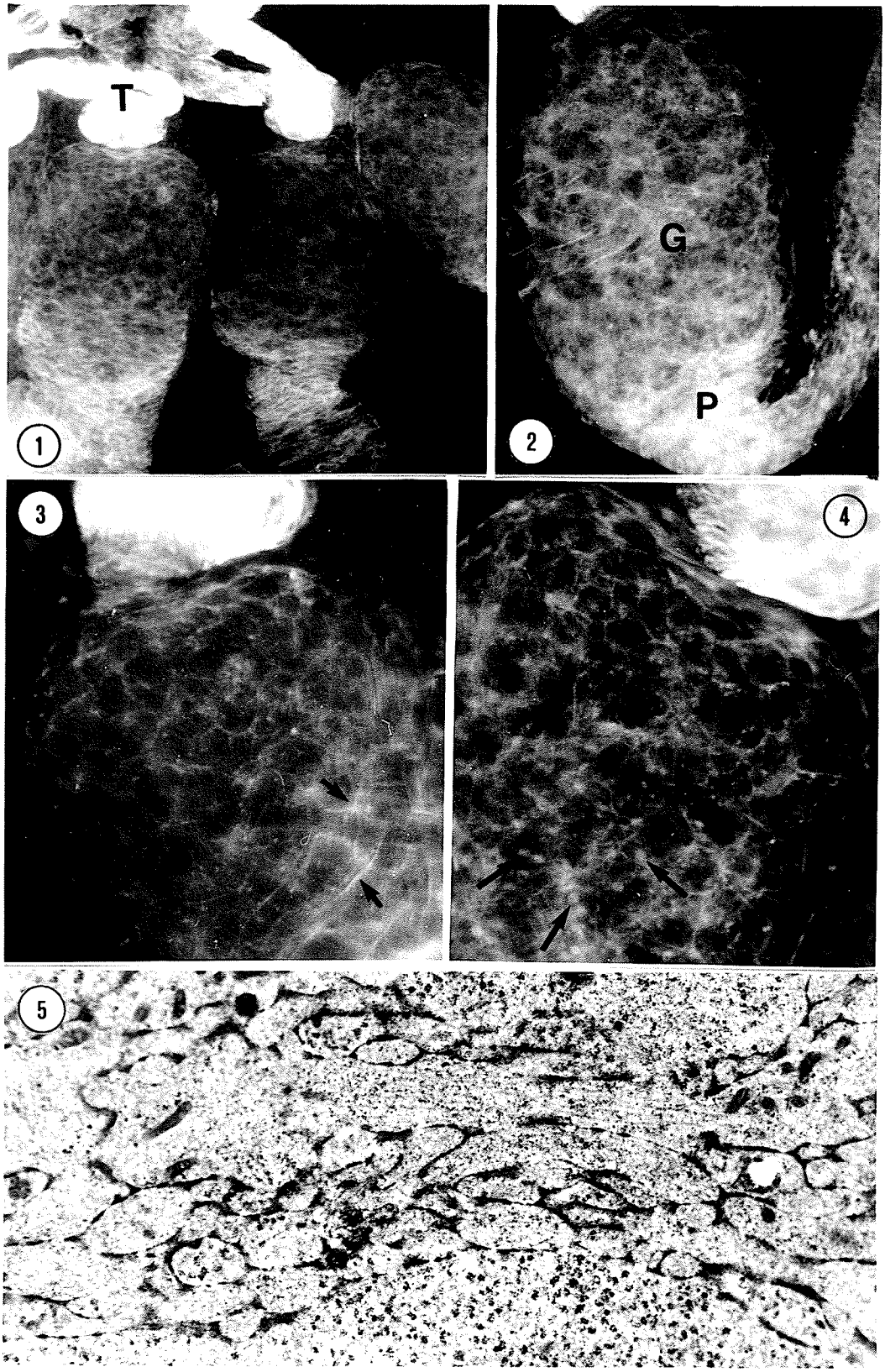
T
1
G
P
2
3
4
5

Plate 2.

Ring canals in the early 5th instar ovariole

Figs. 6 & 7.
Low and high magnification TEMs of the germ cells in the anterior portion of the germarium. Note the various ring canals (arrows) seen in this tangential section. There is electron-dense material associated with the membrane of the bridges.
11,500X; 39,000X

Fig. 8.
Rhodamine-phalloidin staining reveals more prominent ring canals by 6 dpf. Arrows highlight the ring canals.
1,500X

Fig. 9.
High magnification TEM view of an intercellular bridge. Note the membrane densities (arrows), the mid-body remnant (*) and microtubules (M) within the bridge.
38,100X

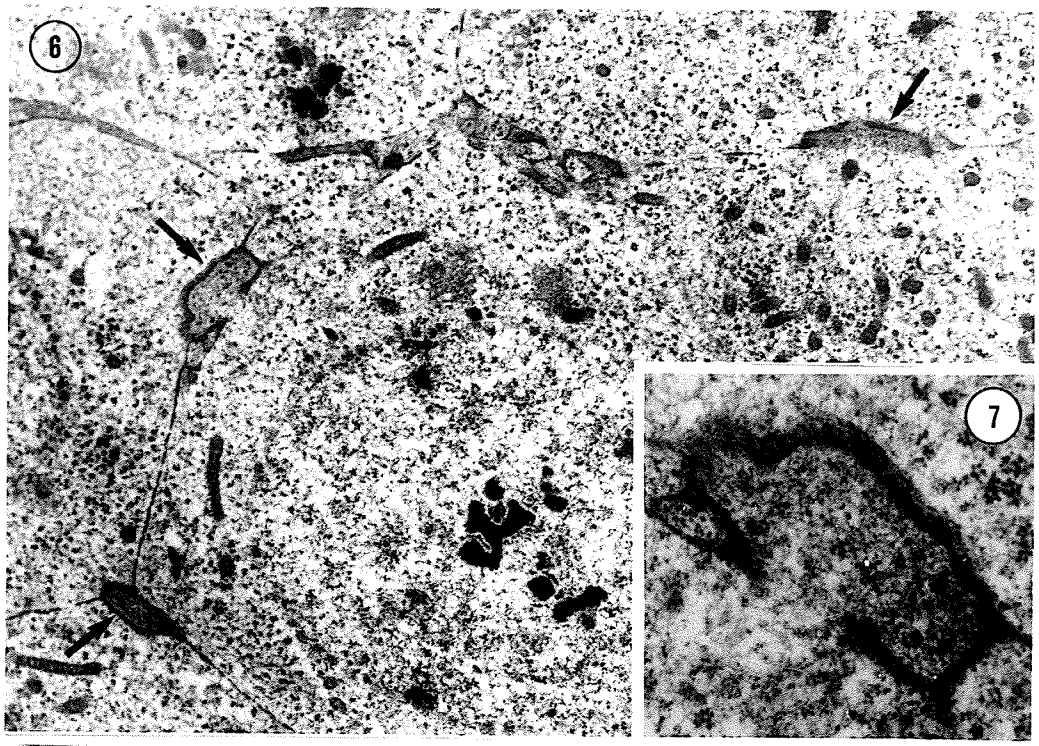
6

7

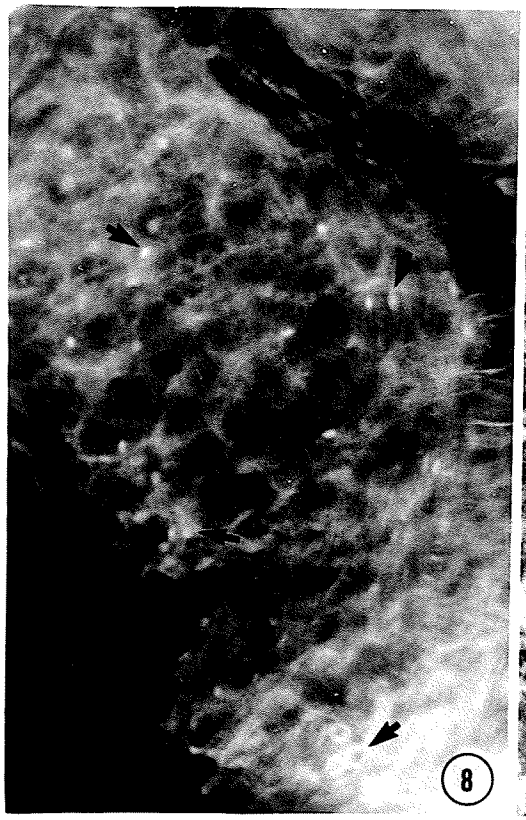
8

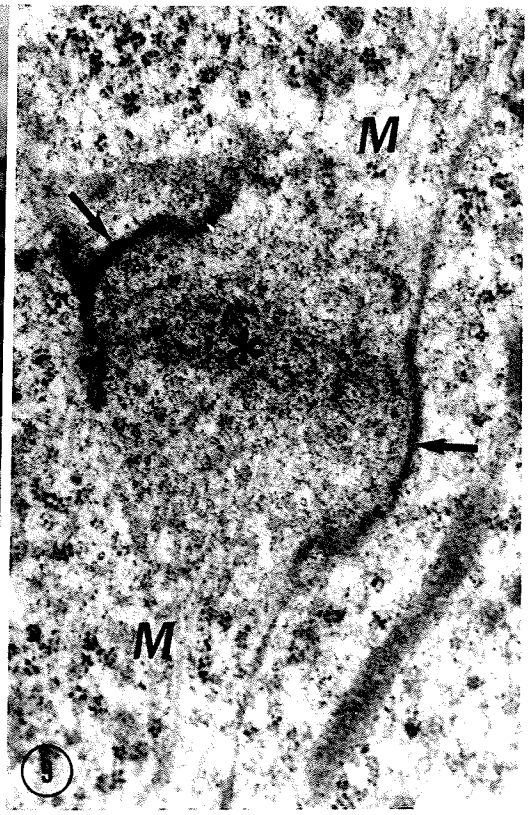
M
M
9

Plate 3.

Ring canals increase during the proliferative phase

Figs. 10 & 11.
Rhodamine-labelled phalloidin stained whole mounts. Numerous ring canals are visible in the germarium. Clusters of ring canals are easily resolved using conventional microscopy due to their thickening F-actin-positive borders.
1,250X; 1,400X

Fig. 12.
TEM of a newly-formed ring canal cluster that contains the fusome (*). The fusome has a distinct, fibrogranular appearance that distinguishes it from the surrounding cytoplasm. This organelle- and membrane-free region of cytoplasm extends throughout the lumen of these three intercellular bridges.
11,250X

Fig. 13.
TEM of a ring canal cluster (arrows). Ring canals at this stage are more electron-dense than earlier stages.
15,300X

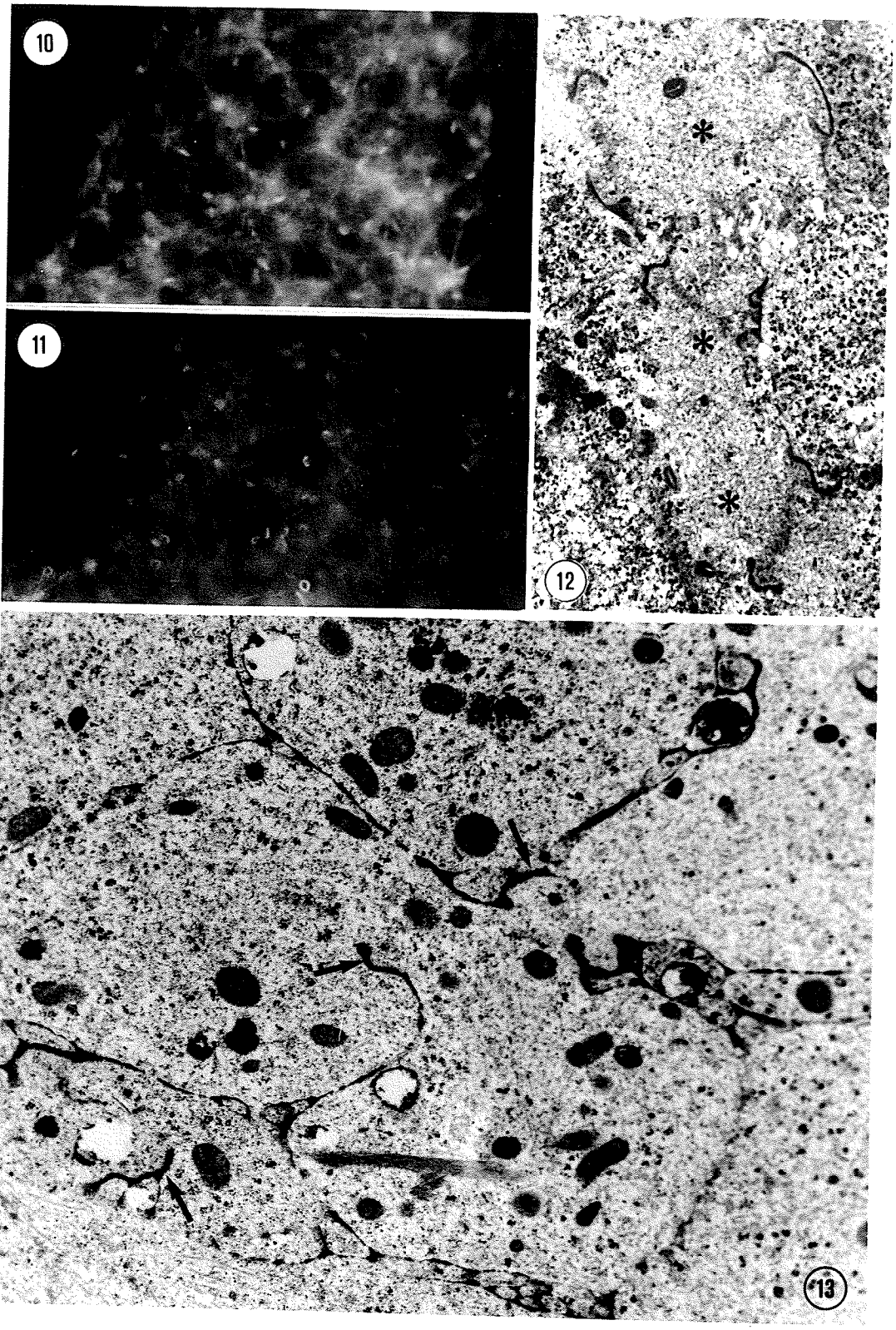
10
11
12
13

Plate 4.

Ring canals of the early differentiation phase

Figs. 14 & 15.
At 12 dpf, rhodamine-labelled phalloidin staining reveals the very distinct F-actin rings of intercellular bridges, even with the general increase in tissue mass and background actin. Fine F-actin struts (arrows) are now visible in the germarium.
2,000X; 2,000X

Fig. 16.
TEM of a cluster of ring canals shows the thick, electron-dense rims (arrows) that are characteristic of intercellular bridges by 12 dpf.
20,500X

Fig. 17.
At 14 dpf, brightly fluorescent circular profiles appear in the rhodamine-labelled phalloidin stained germarium. Some of these actin spots appear donut-shaped, resembling thickened ring canals. The short actin struts appear thicker (arrows).
2,000X

Fig. 18.
Lower magnification view of the rhodamine-labelled phalloidin-stained F-actin structures at 14 dpf. The thicker, larger actin profiles are more prevalent in the basal region of the germarium.
600X

Fig. 19.
TEM of the developing trophic core at 14 dpf. Profiles of intercellular bridges (arrows) are clearly visible within the larval trophic core.
15,200X

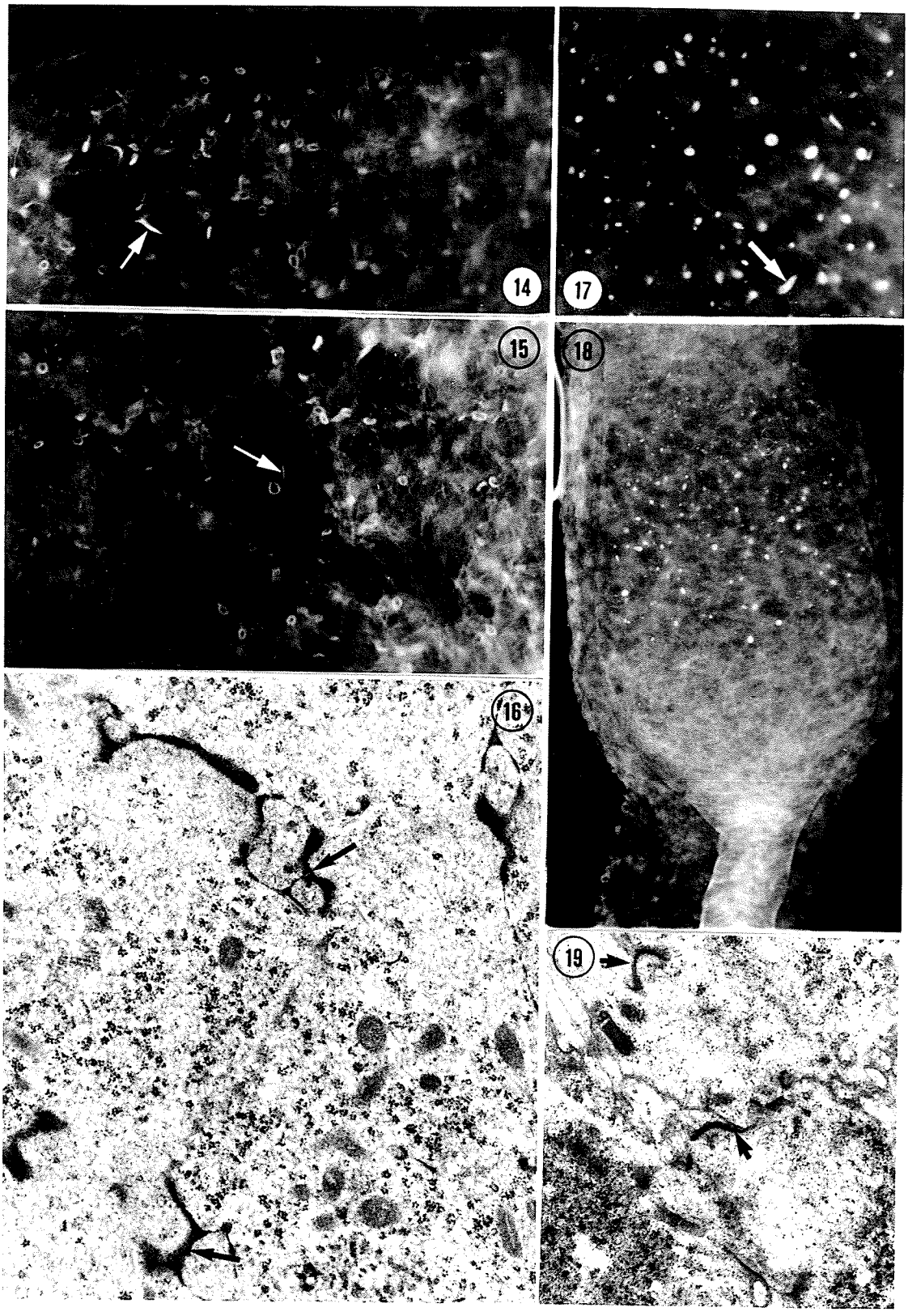
14
17
15
18
16*
19

Plate 5.

Ring canals thickening during the early differentiation phase

Fig. 20.
High magnification TEM view of an intercellular bridge in cross-section. By 14 dpf, the electron-dense component of the bridges becomes thicker. This thickening fibrous material extends laterally away from the bridge itself (arrows).
60,900X

Figs. 21 & 22.
The electron-dense deposits extend along the membranes adjacent to the bridge. The material appears to extend from the bridge into the adjacent membranous area.
18,900X; 25,200X

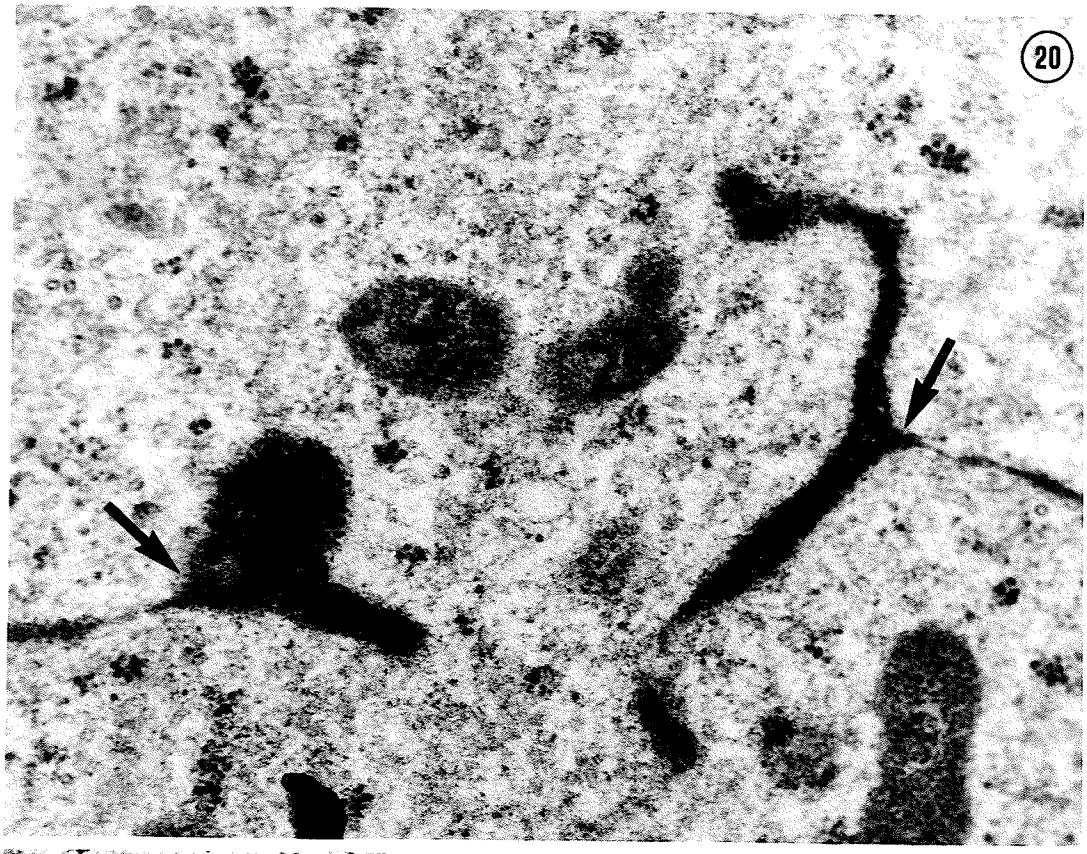
20

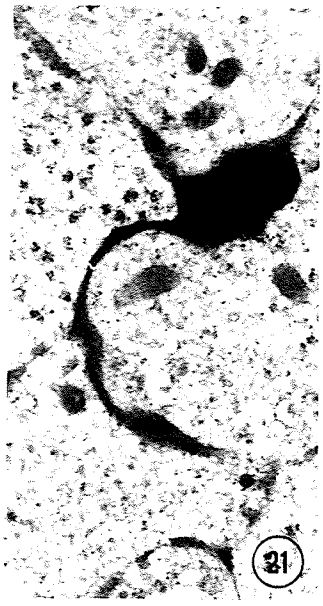
21

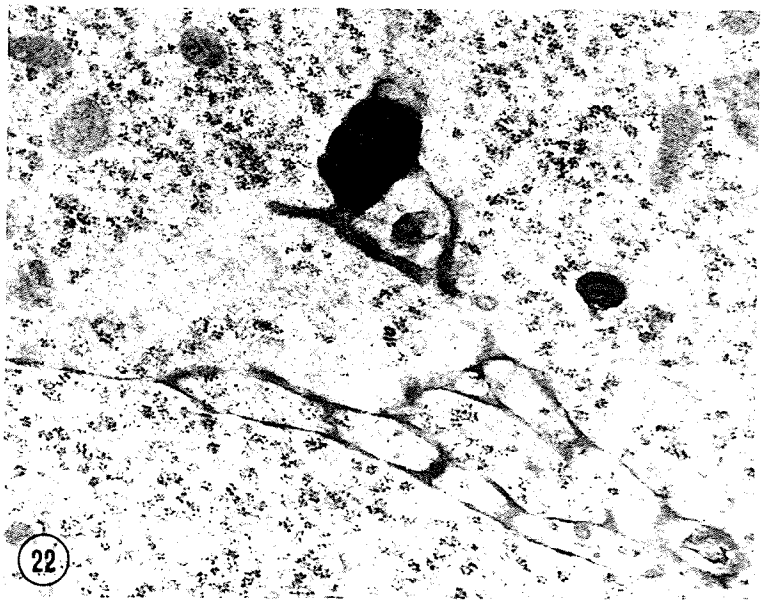
22

Plate 6.

Thickening intercellular bridges

Fig. 23.
Longitudinal TEM section showing 2 adjacent ring canals. At 12 dpf, these ring canals can be distinguished by their characteristic electron-dense memrbane outlies.
12,800X

Fig. 24.
This intercellular bridge is located at the posterior area of the developing trophic core of a 14 dpf ovariole. The lateral edges of the bridge contain a thicker layer of electron-dense material (arrows). Intercellular bridges that occur at the posterior region of the trophic core are usualyy located in a membrane-free area, such as this. The surrounding cytoplasm is a relatively uniform matrix composed of ribosomes and mitochondria.
15,300X

Fig. 25.
This TEM illustrates that the fibrous rim of this ring canal is of uniform thickness.
19,200X

Fig. 26.
This TEM shows a circular, fibrous structure in the basal area of the germarium. Note the prominent thickening of the fibrous ring and the loss of associated membranes.
12,000X

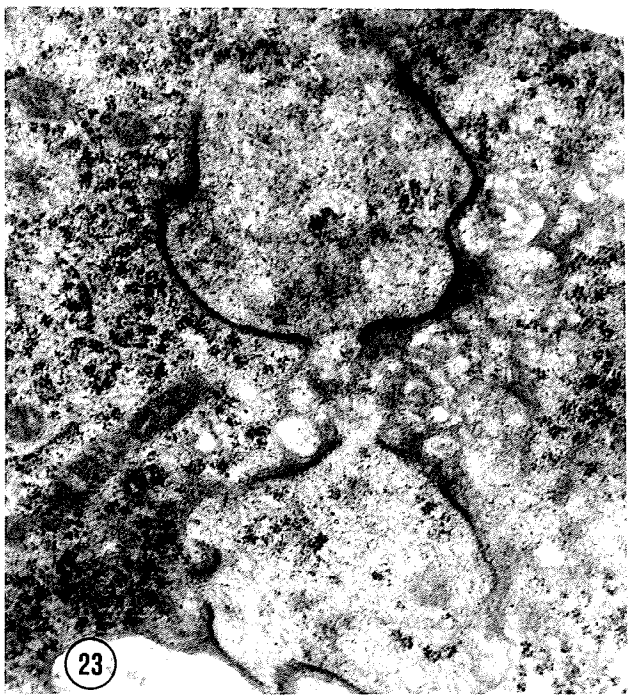
23

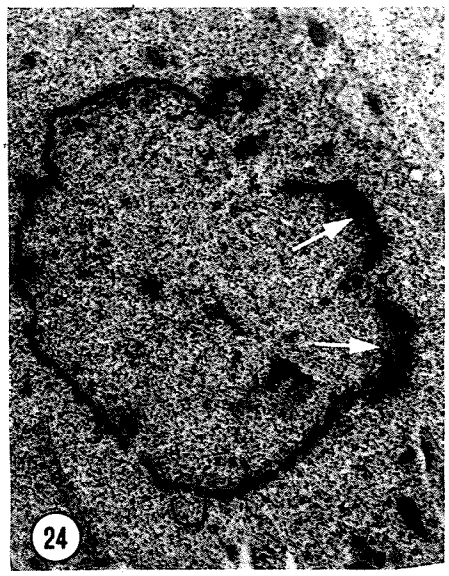
24

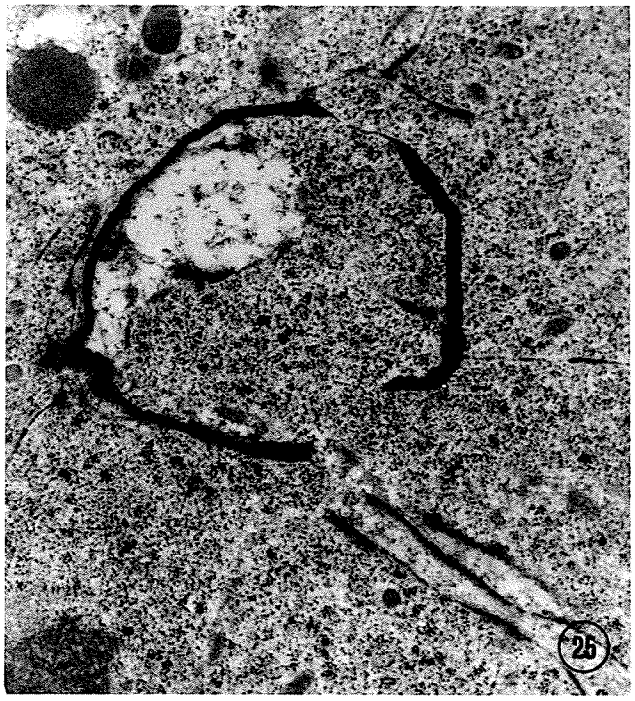
25

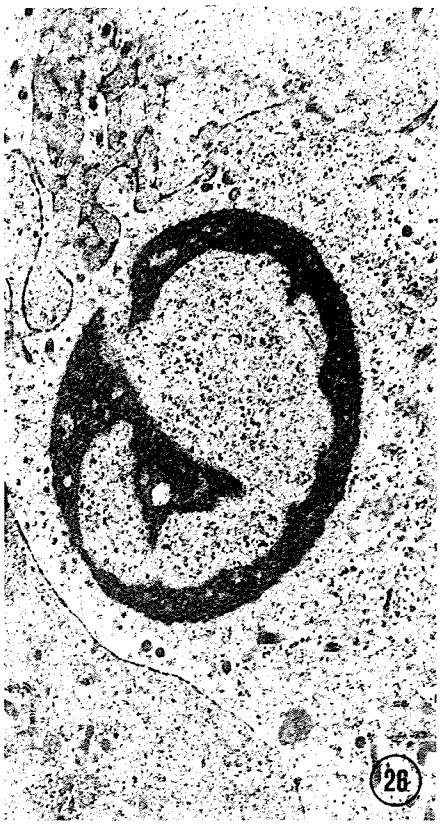
26

Plate 7.

Thickening and reorganization of the fibrous rings during the late differentiation phase.

Figs 27 & 28.
The thickened ring canals seen in these fluorescence micrographs of phalloidin-stained whole mounts retain their circular profile (hollow arrows); the lumen of these intercellular bridges have become "filled in" with actin. Short, thick, actin struts are present throughout the germarium, some seen extending from ring canal structures (small arrows).
3,000X; 3,000X

Fig. 29.
This micrograph shows the various stages of thickening from an early fibrous ring (*) to a thickening one.
13,100X

Fig. 30.
This TEM section reveals the fibrous, granular nature of the actin structures in the developing trophic core.
26,400X

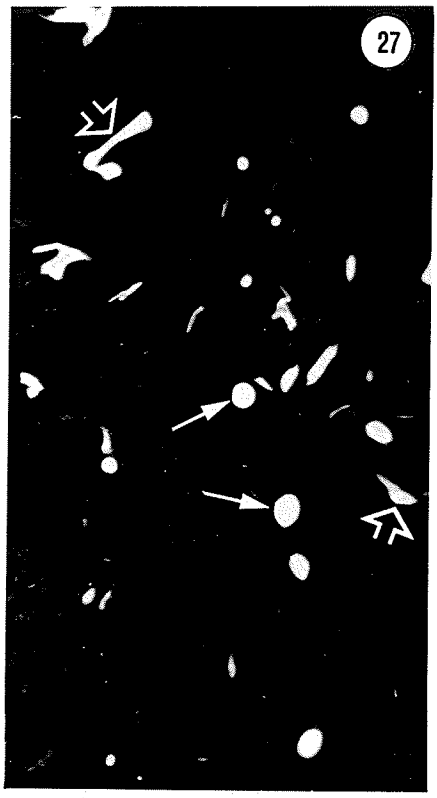
27


28


29

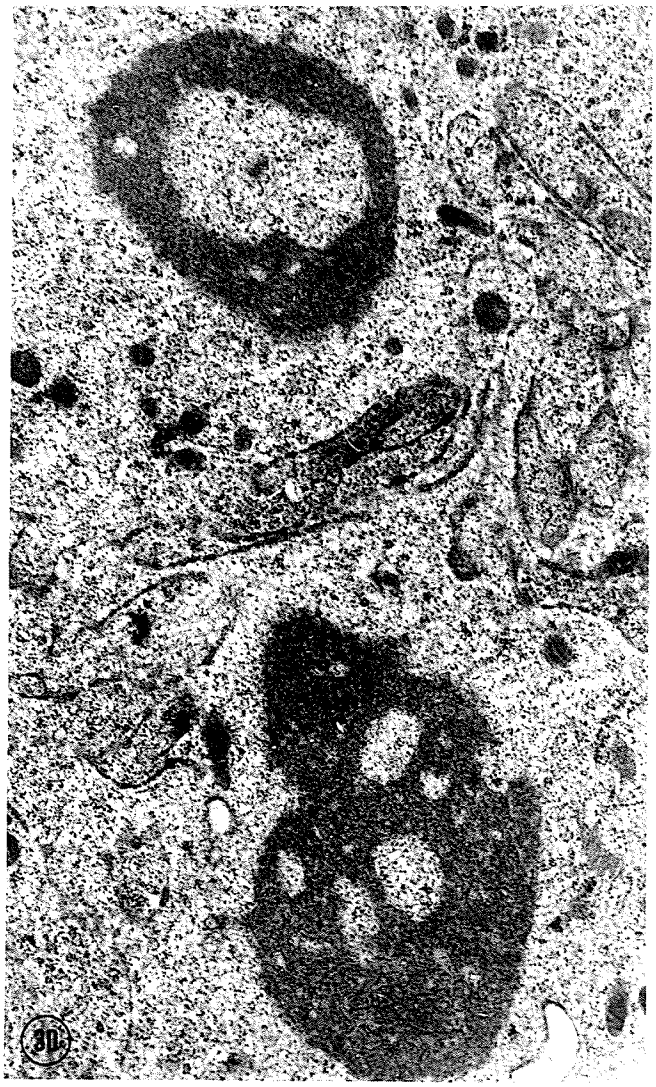
30

Plate 8.

Visualization of F-actin structures enhanced by deconvolution.

Figs. 31 & 32.
These figures compare the fluorescence images before and after deconvolution. Fig. 31 illustrates the non-deconcoluted image of a rhodamine-labelled phalloidin stained ovariole (7 dpf). A cluster of ring canals (* and higher magnification inset) is barely visible. Fig. 32 shows that deconvolution improves the clarity of the ring canal cluster. The circular structures are now clearly visible as rings, with distinct, hollow centres (* and higher magnification inset).
3,000X (both figs.); 4,500X (insets)

Figs. 33 & 34.
Fig. 33 is a non-deconvoluted image of thickened, enlarged ring canals at 19 dpf. In this micrograph, they are visible as bright, circular fluorescent profiles. Background fluorescence and the strong fluorescence signal from the ring canals themselves prevents resolution of fine detail, even at higher magnification (inset) in a different preparation. Deconvolution of these images in Fig. 34 reveals the donut-shaped profiles of the thickened intercellular bridges. The hollow profiles of elongating ring canals are also visible (*).
2,000X (both figs.); 5,000X (insets)

Figs. 35 & 36.
The branching and banding of the phalloidin stained F-actin mesh of the adult tropharium is evident in the standard fluorescence image (Fig. 35), but even these well-developed structures (particularly the fine branches and banding pattern) are more clearly visible after deconvolution (Fig. 36).
2,250X (both figs.)

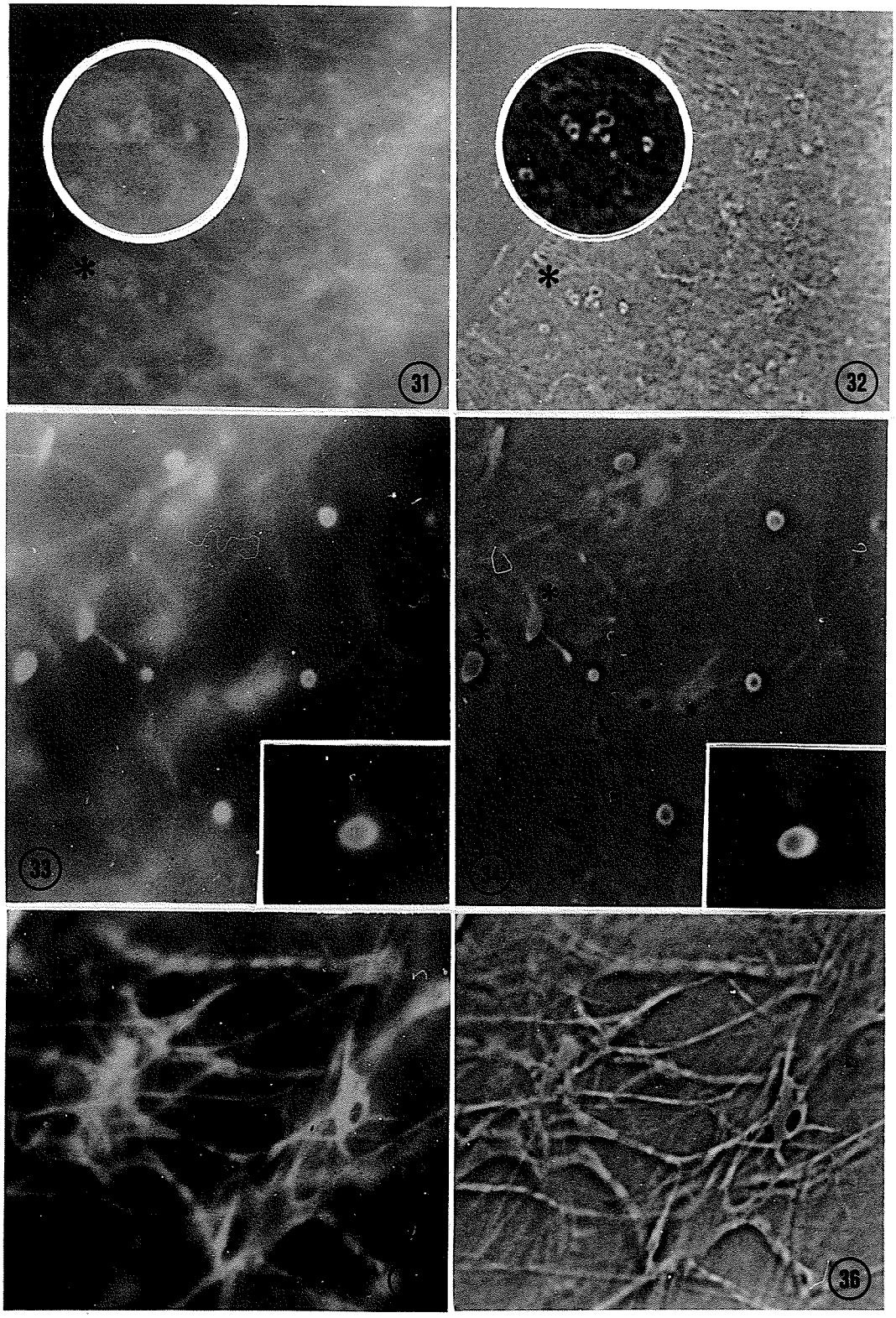
31
32
33
36

Plate 9.

Morphology of the F-actin struts during the late proliferative phase

Fig 37.
This TEM illustrates the thick and fibrous nature of the ring canals within the trophic core and growing extensions.
33,500X

Fig. 38.
Immunogold visualization of anti-actin antibodystaining of TEM sections verifies that the fibrous structure stains positively, as shown here. Note that the 10-nm gold particles only label the fibrous structure.
34,500X

Figs. 39 & 40.
The growth and increasing complexity of the actin in the basal area of the germarium is seen in these phalloidin stained fluorescent preparations. The actin struts vary in thickness and length. Fibrous, circular ring canals are present throughout the germarium.
750X; 1,500X

Figs. 41 & 42.
Thin sections of the ovariole at 19-20 dpf reveal various profiles of the elongating fibrous structures within the trophic core area. They are no longer associated with membranes.
17,000X; 16,000X

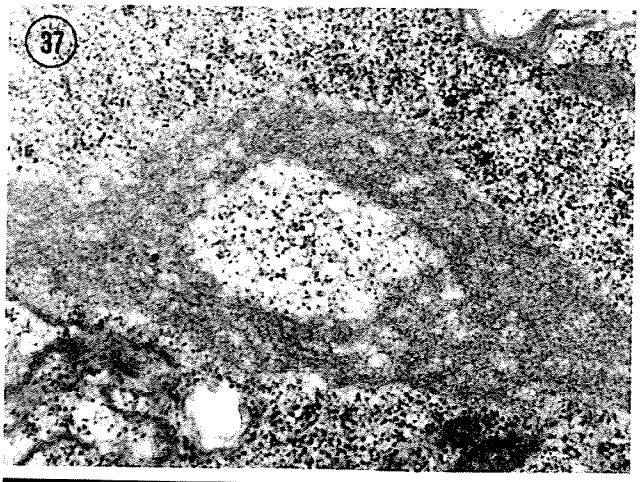
37

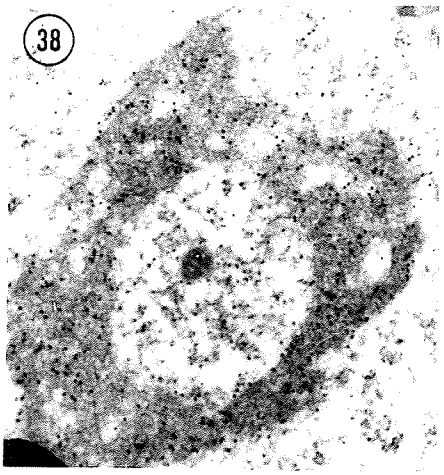
38

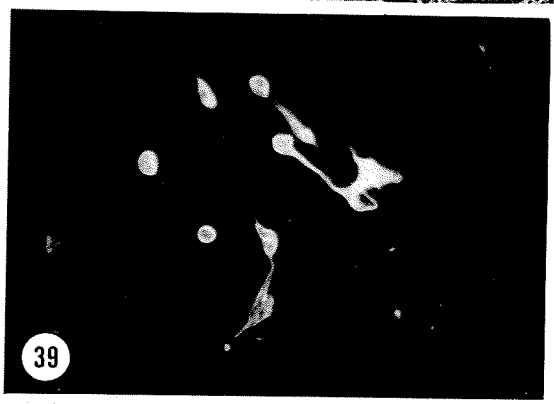
39


41


40

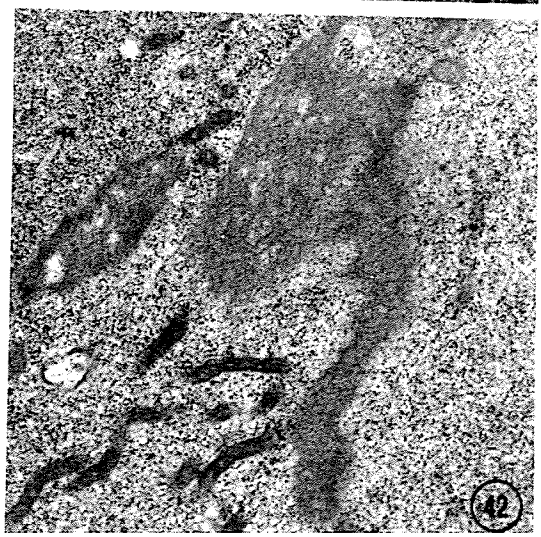
42

Plate 10.

Structure of the late pre-molt F-actin array

Figs. 43 & 44.
Low and high magnification fluorescence micrographs of the positively-staining F-actin mesh. The interconnecting struts in the basal area of the tropharium lengthen and the complexity of the organization increases.
800X; 2,500X

Fig. 45.
This TEM shows a part of the complex fibrous branching network.
28,300X


43


44

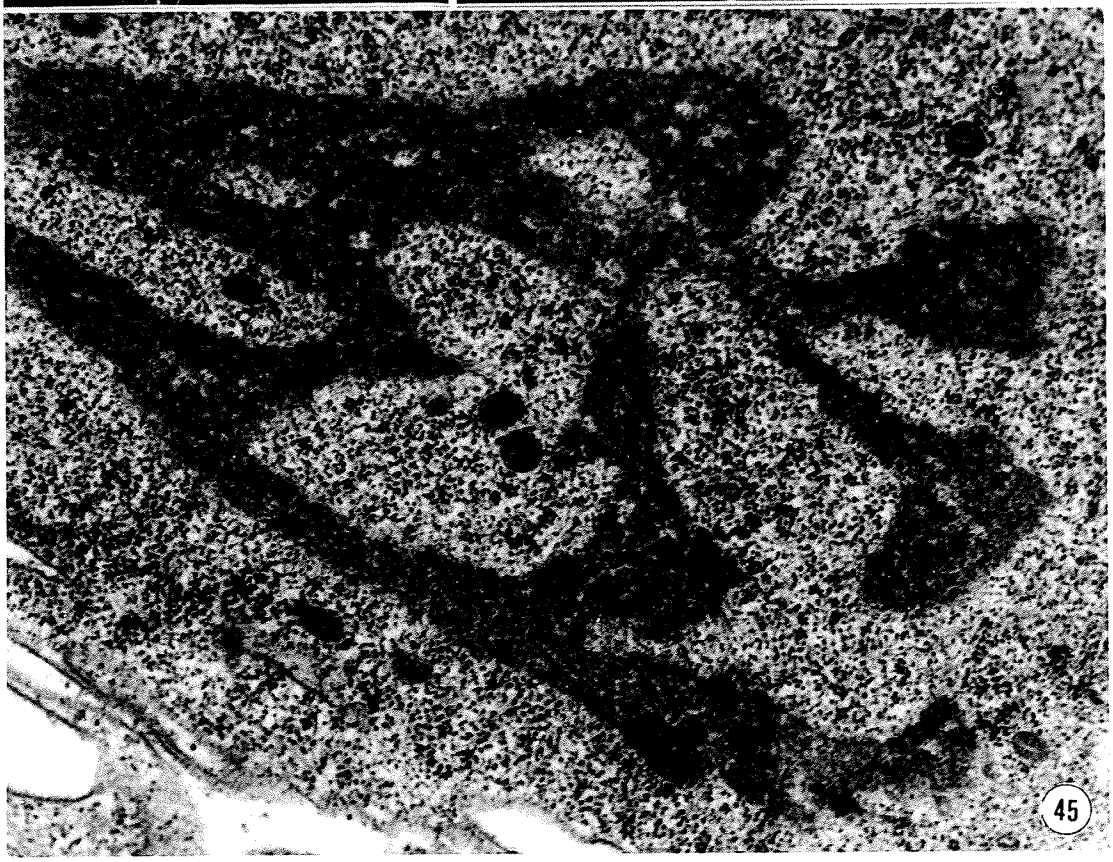
45

Plate 11.

The F-actin mesh in the newly-emerged adult.

Figs. 46 & 47.
These two micrographs illustrate anti-actin immunostaining of the fibrous structures seen in TEM, as visualized with 5 nm gold-labelled secondary antibody. Gold label is only seen over the fibrous structures. The gold-labelled secondary antibody is localized to the fibrous actin struts in the trophic core region.
39,100X; 54,000X

Figs. 48 & 49.
These fluorescence micrographs of the phalloidin-stained F-actin mesh in a newly-molted adult illustrate the spectacular array of F-actin fibers encircling the posterior region of the trophic core. At the anterior portion of the tropharium, thickened ring canals and shorter actin struts are present. As the core completes its morphogenesis to the final adult structure, the struts elongate and interconnect to produce the complete actin mesh.
800X; 1,500X

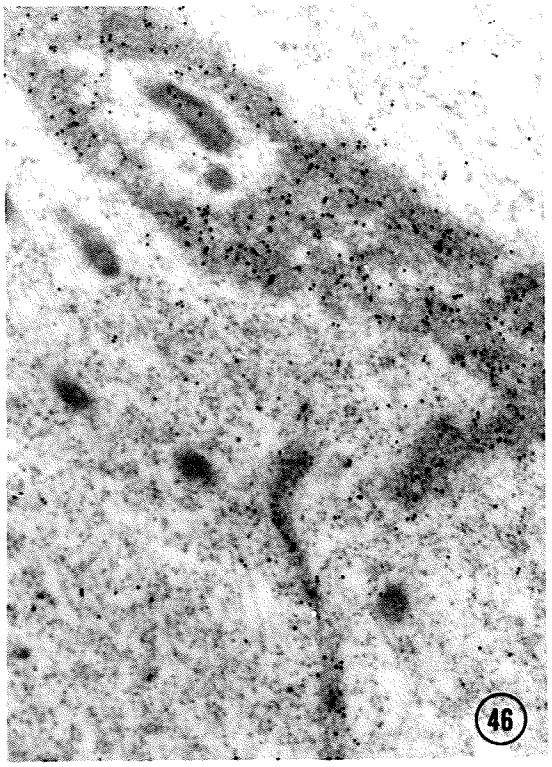
46

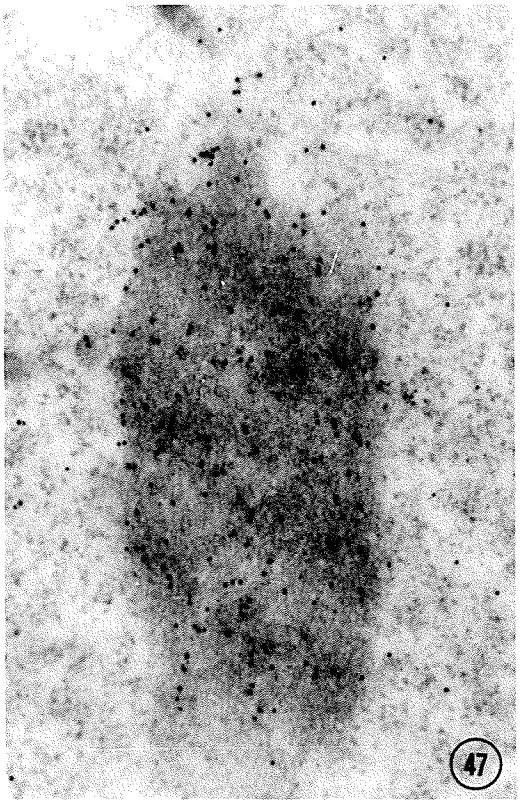
47

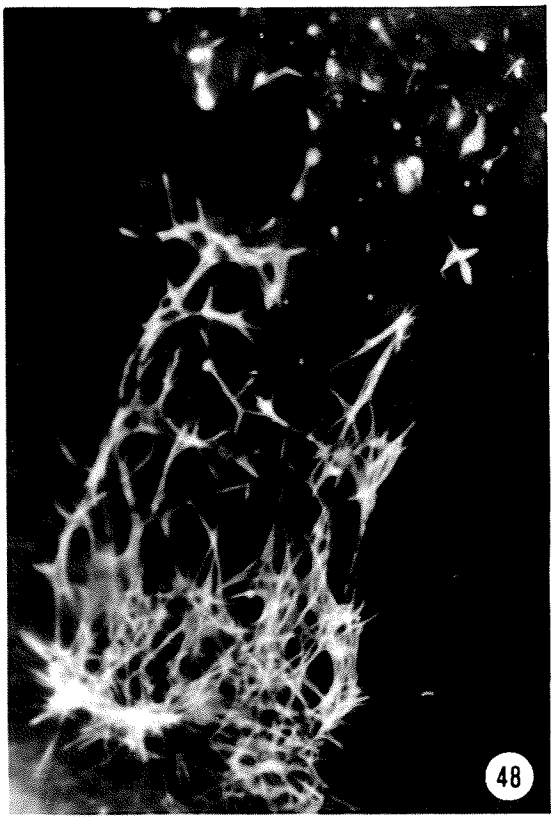
48

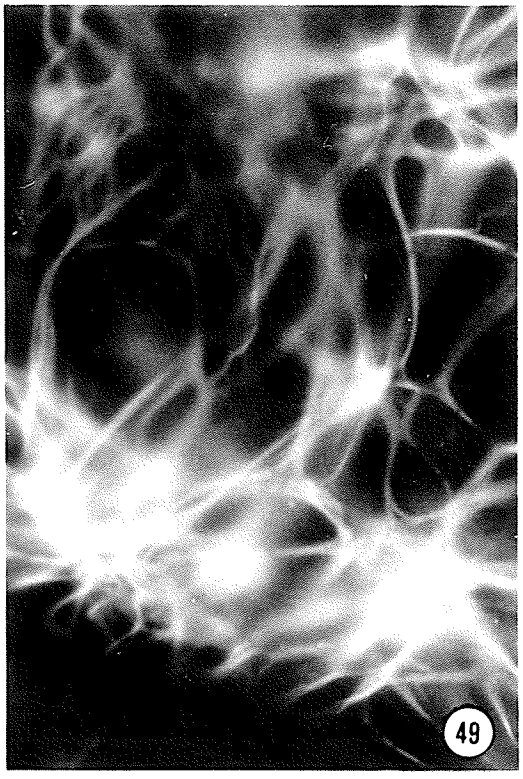
49

DISCUSSION

Research on meroistic insect ovaries has contributed significantly to our understanding of many fundamental processes in developmental biology. The polytrophic and telotrophic systems are both excellent experimental models for studying the role of cytoskeletal elements in oogenesis. Polytrophic and telotrophic ovaries differ developmentally and structurally; however, the establishment of structural and functional polarity within the nurse cell-oocyte syncytium is a fundamental aspect of oogenesis in both systems. Microfilaments in the *Drosophila* egg chamber orchestrate basic cellular processes (oocyte differentiation, intercellular transport, maintenance of structural integrity in the egg chamber) which are an essential prelude to the production of a functional, mature oocyte. *Drosophila* oogenesis has emerged as a dynamic and versatile model for examining the functions of the actin cytoskeleton during development, in particular, the development and function of ring canals in maintaining normal nurse cell-oocyte interaction.

The hemipteran telotrophic ovary is characterized by an even more exaggerated structural and functional polarity. Analysis of numerous insects with telotrophic ovaries reveals that actin is a common feature of nurse cells (Gutzeit and Huebner, 1986; Huebner and Gutzeit, 1986). In the adult telotrophic ovary, the actin mesh separates the synthetically active nurse cell lobes from the microtubule-rich central trophic core (Huebner and Gutzeit, 1986). This actin mesh is

characteristic of the hemipteran telotrophic ovary, and is not present in the polytrophic ovary. The function of the actin cytoskeleton in the telotrophic ovary is unknown. Now that the functional role of actin in the polytrophic ovary are becoming clearer, it is particularly important to learn whether the functions of the actin cytoskeleton as seen in *Drosophila* oogenesis are conserved in the structurally more complex telotrophic ovariole.

In this study I demonstrated that the F-actin mesh in the trophic core of the *Rhodnius* telotrophic ovariole originates from the F-actin rings of intercellular bridges, or ring canals. These F-actin rings provide nucleation sites for the assembly of the elongated actin struts which form the actin mesh surrounding the adult trophic core. Results from rhodamine-labelled phalloidin staining, in the context of TEM observations, indicate that the ring canals provide the focal points for actin polymerization, initially thickening and finally forming projections that branch and elongate. F-actin assembly begins at the rim of the ring canals, gradually expanding along the adjacent membranes. As membrane fusions and restructuring occurs in the germarium, thickened ring canals dissociate from the cell membranes, but remain intact, allowing for further actin polymerization along their surfaces. The coincidence of fibrous rings free of membranes, along with the membrane restructuring in the germarium, supports the conclusion that a developmental continuum exists from the thickened ring canals to the fibrous actin rings. Although some of the circular, fibrous actin structures may be cross sections of longer, hollow actin struts, serial sections in EM demonstrates that these

structures do represent the circular actin profiles seen with fluorescence microscopy. Immunocytochemistry using anti-actin antibody visualized with colloidal gold-conjugated secondary antibody verified the F-actin composition of these fibrous structures.

By utilizing the combination of fluorescence and electron microscopy, the changes in the F-actin pattern in whole, permeabilized ovarioles could be observed throughout the various developmental stages. A comparison of results obtained through both these methods enables the 3-dimensional visualization of the complex developmental changes that occur during the formation of the F-actin mesh. Phalloidin is a specific probe for F-actin, and no cross-reactivity with other cytoskeletal proteins is known (Faulstich et al., 1993). The phalloidin staining observations on the 5th instar ovarioles provides an overall picture of the location and structural changes that occur in the F-actin pattern of the developing ovarioles. TEM supports the fluorescence results and provides additional information on the ultrastructural changes that occur as the ring canals thicken and elongate.

The results of this study are significant because 1) a developmental analysis of the F-actin mesh provides an initial step in elucidating its function in the telotrophic ovariole, and 2) the F-actin rings of intercellular bridges function as nucleating sites for actin assembly, indicating a possible mechanism for the formation of such a complex actin-based structure.

In order to understand the mechanism of the actin mesh formation, one should consider the origin of the nurse cell-oocyte syncytium as proposed by

Huebner and Anderson (1972). The syncytial arrangement of the adult ovariole arises from the fusion of separate syncytial germ cell clusters. The larval trophic core consists of a complicated array of cell processes (Huebner and Anderson, 1972; Lutz and Huebner, 1981). Cytoplasmic extensions from nurse cells are continuous with some processes of the core. The core remains connected with the developing nurse cells through intercellular bridges. Numerous bridge profiles are visible within the core itself. The core remains connected with developing nurse cell clusters through intercellular bridges. Numerous bridge profiles are visible within the core itself. Small, microtubule-filled cords connect the oocytes to their respective sibling cell clusters (Valdimarsson and Huebner, 1989). It is well-known that the development of actin and microtubular arrays exert regulatory influences on each other (Goslin et al., 1989; Lin and Forscher, 1993; Langford, 1995). Although it is unknown whether the development of the F-actin mesh in *Rhodnius* is affected by the microtubule distribution, the development of the actin struts must be visualized in context of the structural reorganization of cell membrane fusions and microtubule formation that occurs in the developing trophic core.

As the core continues to develop, membrane fusions and restructuring could provide additional actin for assembly at the ring canal nucleation sites. The ring canals appear to be exempt from membrane fusions; they remain intact despite the plasma membrane restructuring that occurs throughout the larval trophic core. Thus, the actin filaments of the intercellular bridges must be highly stabilized in order to withstand the massive regional restructuring occurring in the

germarium. Their stability and abundance throughout the developing germarium makes the intercellular bridges convenient sites for controlled actin assembly.

Studies in other eukaryotic organisms indicate that the formation of actin cytoskeletal structures begins at distinct, nucleating sites in the cell (Barkalow and Hartwig, 1995). The study of the acrosomal process in *Limulus* and *Thyone* sperm (Way et al., 1995), the mating tubule in *Chlamydomonas* (Barkalow and Hartwig, 1995), and the "rocket tail" of *Listeria* (Southwick and Purich, 1994) show that actin formation begins at discrete locations in the cell. In platelets, neutrophils, fibroblasts, and mammalian liver cells, actin assembly following activation occurs on the exposed barbed ends of pre-existing actin filaments (Tranter et al., 1991; Symons and Mitchison, 1991; Cao et al., 1993). The cell membranes of *Dictyostelium* are able to induce the formation of stable actin trimers and thereby nucleate actin assembly (Shariff and Luna, 1990; Chia et al., 1993). The dissociation of actin filament capping proteins, such as CapZ, from the barbed ends of actin filaments results in actin polymerization at the leading edge of motile pseudopods (Symons and Mitchison, 1991).

The formation of the F-actin mesh in *Rhodnius* provides the first evidence that the F-actin structures arise from the F-actin rings of ring canals. Ring canals, or intercellular bridges, were initially thought to function in synchronizing germ cell division (Zamboni and Gondos, 1968). As a result of incomplete cytokinesis during mitotic divisions, male and female gametes develop as a syncytium, with each cluster of germ cells interconnected by cytoplasmic bridges. In some invertebrates,

intercellular bridges enable the transport of nutrients from nurse cells to the oocytes (Anderson and Huebner, 1968; Huebner, 1984; Huebner et al., 1993; Robinson et al., 1994).

Recent studies of *Drosophila* oogenesis have begun to paint a picture of even more active and fundamental roles played by ring canals. Ring canals regulate the transport of materials from the nurse cells to the oocyte (Yue and Spradling, 1993; Xue and Cooley, 1993). Equally important is the role played by ring canals in oocyte differentiation. In developing cystocytes, the fusome forms from the remnants of the mid-body, and is thought to stabilize the ring canals. Branches of the fusome (also known as polyfusome) interconnects pre-existing ring canals. The unequal distribution of the polyfusome throughout the syncytial germ cell cluster is thought to generate asymmetry in an otherwise identical cluster of germ cells, and this asymmetry appears to be a critical factor in oocyte determination. One of the two cells with four ring canals and their accompanying portions of the polyfusome differentiates into the oocyte (King et al., 1982; Spradling, 1993).

Despite these intensive studies, little is known about the organization and function of intercellular bridges at the molecular level. Information on the way the actin filaments associate with the plasma membrane of ring canals is beginning to emerge. In *Drosophila*, ring canal actin filaments are oriented circumferentially and attached to the plasma membrane at the periphery of each intercellular bridge (Tilney et al., 1995b). The actin filaments are initially oriented in mixed polarities,

similar to the contractile ring in cytokinesis. The contractile ring in cytokinesis is a transient, bipolar array of actin filaments with their barbed ends attached to the plasma membrane at sites around the equator of a dividing cell (Satterwhite and Pollard, 1992). Throughout development, the ring canals increase in size and the actin filaments undergo a reorganization. From stages 5 onwards, the actin filaments form a net of parallel, circumferentially oriented, interconnected bundles (Tilney et al., 1995b). The actual density of the actin filaments remains unchanged throughout development.

Although the polarity of the ring canal-associated actin filaments is unknown in *Rhodnius*, it is highly likely that the filaments are reorganized throughout the development of the actin mesh. The F-actin filaments associated with the membranous component of intercellular bridges may provide the necessary accumulation of actin filament barbed ends to promote the further assembly of F-actin at these sites. In the formation of the F-actin array in the *Rhodnius* tropharium, the membranous component of each ring canal may fuse with the surrounding membrane and cell processes in the reorganization of the larval trophic core. In the absence of the membrane attachment, the barbed ends of actin filaments become exposed, thereby creating sites for further actin polymerization. Alternatively, the actin filaments in the ring canal may undergo a reorganization, so that more "free" barbed ends are created for actin polymerization. This may explain why the thicker ring canals in the later developmental stages appear more fibrous and less electron-dense than those of

the early proliferative stage. The organization of the actin filaments may have to be constantly modified to facilitate the sequential addition of actin monomers to the elongating actin structures. Cao and Wang (1990) have suggested that pre-existing actin filaments are recruited in the formation of the contractile ring, probably through movement and reorganization. The formation of the F-actin mesh in *Rhodnius* may occur by a similar mechanism. The F-actin filaments associated with cell membranes may be recruited to the ring canal nucleation sites during the massive cellular reorganization that occurs in the larval tropharium. It is possible that membrane-associated actin filaments move towards the ring canals in a mechanism similar to cortical flow (Bray and White, 1988).

The stability of ring canals suggests that their actin filaments are stabilized and/or crosslinked by actin-binding proteins. Recent work has shown that cleavage furrows of dividing cells are associated with numerous actin-binding proteins (Sato et al., 1991; Satterwhite and Pollard, 1992; Field and Alberts, 1995). It is likely that these, or other, proteins are associated with the ring canals and participate in stabilizing the F-actin rings in *Rhodnius*. Ring canal morphogenesis in *Drosophila* is now known to be a complex and highly regulated process (Robinson et al., 1994). The sequential addition of phosphotyrosine, actin, hts, and kelch are critical for normal ring canal morphogenesis and function. In *Drosophila*, the compaction of the ring canal-associated proteins in the later stages of oogenesis can be observed ultrastructurally (Yue and Spradling, 1992). In contrast, the ring canals in *Rhodnius* appear to become less "compact" as development progresses. The

texture of the ring canals becomes more fibrous and less electron-dense than ring canals of the earlier stages. The reorganization of the actin filaments around the ring canals is likely accompanied by the addition and/or modification of actin-associated proteins.

Attempts to localize *Drosophila* actin and ring canal-associated proteins (hts, kelch, chickadee, and singed) in *Rhodnius* thus far have been unsuccessful. The monoclonal antibodies to the *Drosophila* proteins may not have recognized epitopes on homologous proteins in *Rhodnius*. Problems with antiobody penetration cannot be ruled out, due to the size and complexity of the *Rhodnius* ovariole. It is also possible that these proteins are not present in *Rhodnius*. Previous biochemical studies of actin in *Rhodnius* germ tissue revealed that the actin had an unusually high molecular weight (63 kD, as compared to 43 kD for other actin isoforms) (Kelly, 1989). The approximately 20kD of additional material present on the actin molecule may be the reason why *Rhodnius* actin cannot be purified using routine DNase I chromatography (Kelly, 1989). This unusual actin molecule may be post-transcriptionally or pre-translationally modified (Kelly, 1989); it is possible that the proteins associated with *Rhodnius* actin may be modified to regulate the assembly and organization of this unusual molecule. Therefore, antibodies to "conventional" actin-binding proteins may not be able to recognize homologous proteins in *Rhodnius*. Further biochemical analysis is necessary of actin and its associated proteins in the *Rhodnius* ovariole.

The thick actin struts in the tropharium display a distinct banding pattern,

indicating that they are cross-linked by one or more actin-binding proteins. The banding pattern is not initially visible in the short, newly formed actin struts. However, the longer and more branched actin struts in the basal region of the pre- and post-molt ovariole begins to exhibit the banding pattern, indicating that the more mature actin struts undergo yet another reorganization. The cross-linking of the highly stable adult actin struts may be analogous to that of the *Drosophila* bristle (Tilney et al., 1995a; Tilney et al., 1995b). In *Drosophila* bristles, the singed and forked proteins are necessary for bundling the actin filaments together. The forked proteins tie the filaments together early in development. The bundles are later zippered together by the singed protein. These filaments are hexagonally packed and show a 12 nm periodicity in longitudinal section. Each bristle appears to be made up of a number of small actin bundles that come together to form the 7-11 large bundles in the bristle core. The presence of distinct, regular banding pattern in the *Rhodnius* actin struts may be due to the cross-linking of the shorter actin filaments to form the longer, branched ones of the adult. However, the fact that such a pattern is not obvious in the newly-forming actin struts and is only visible in the almost fully-formed actin mesh indicates that a rearrangement of the actin filaments occurs once the final pattern of the actin struts is established in the trophic core. The addition and/or reorganization of actin and its associated proteins may be necessary to further reinforce the long, branched actin struts.

The F-actin network in the trophic core likely functions as a structural support. At the onset of the rapid cytoplasm phase in *Drosophila*, the appearance

of actin fibers in the cytoplasm functions to anchor nurse cell nuclei in place. In a similar manner, the F-actin struts in the trophic core may function to maintain the structural integrity of the syncytium during oogenesis. The F-actin cables are located in the periphery of the core, surrounding the microtubule-laden central area. The role of the actin mesh may be to separate the synthetic compartments (nurse cells) from the transport route to the oocyte (the microtubule-laden trophic core). It is unclear whether the actin mesh undergoes turnover of actin filaments. In the adult ovariole, there are three distinct subpopulations of nurse cells, categorized according to their morphological and functional attributes. Zone I nurse cell, at the apex of the tropharium, are constantly undergoing mitosis to regenerate the nurse cell population. In the adult ovariole, there is always a population of ring canals at the anterior tip of the tropharium. Currently, it is unknown whether these ring canals participate in a dynamic rearrangement of the actin mesh at the anterior tip of the tropharium. Given the length of time and complex cellular restructuring that occurs during the formation of the actin mesh, it is unlikely that the actin struts are turned over on a massive scale. The mid-to-posterior region (Zones II and III) nurse cells are in the process of active synthesis and surround the main body of the trophic core. Therefore, a stable F-actin array could be important in excluding the nurse cell nuclei from the core and act as structural support for the core itself.

It is also possible that some of the finer strands at the periphery of the core function in transporting materials from the nurse cells to the microtubule-laden

central area. Recent work has indicated that organelles have the ability to move along both microfilaments and microtubules (Kuznetsov et al., 1994; Bearer et al., 1993). These fine microfilament networks may not be resolvable by conventional means, such as fluorescence, DIC, or EM. The thickness of the tissue and the prominence of the actin fibers surrounding the trophic core make it virtually impossible to resolve the thinner actin fibers with DIC. Without some new approach, it will be necessary to isolate the F-actin mesh in order to perform motility assays to determine if actin-based motility is present in the tropharium.

Conclusions

This study indicates that the actin borders of intercellular bridges can function as actin-nucleating sites, resulting in morphogenesis of more complex cytoplasmic actin arrays. The telotrophic ovariole, with its highly polarized syncytial structure and rich cytoskeletal composition, provided an excellent system in which to study this process. While the elaborate complexity of the syncytial compartmentalization of the telotrophic ovariole was a complicating factor in this study, it also provided a unique morphogenetic system with many ring canals and enhanced membrane associated actin changes. Elucidating the development of the F-actin mesh is a first step in determining its function in the telotrophic ovariole. Clearly, the F-actin mesh resides at an important location in the tropharium: in between the core and the nurse cell lobes. It is tempting to postulate that the F-actin mesh plays a structural role in maintaining the integrity of the tropharium, thereby facilitating synthesis and transport of materials to the oocyte. However,

very little is known about the biochemistry and molecular composition of the actin mesh. Identifying the actin-binding proteins involved in its formation and maintenance, as well as the polarity of the actin filaments, will be crucial for future analysis of its structure and function. The morphogenesis of the actin mesh in itself provided a unique opportunity for studying the role of ring canals as nucleation sites for further actin assembly. The F-actin mesh provides a useful model for studying cytoskeletal morphogenesis and function during the development of the structurally polarized telotrophic ovariole.

APPENDIX I

BACKGROUND

Actin: General Background and Biochemistry

Actin is one of nature's most abundant cellular proteins (Pollard 1981), and is highly conserved amongst different organisms (Bershadsky et al., 1995). Nonmuscle cells achieve a wide variety of shapes by organizing their cytoplasmic actin filaments into various structures (Bretscher, 1993). The plasma membrane of eukaryotic cells is intimately associated with cortical microfilaments that not only define its shape, but also participate in many membrane-based processes - cell locomotion, cytokinesis, transmembrane signalling, phagocytosis, endocytosis, and exocytosis - to name a few (Cramer et al. 1994). It is now understood that organelle motility in eukaryotic cells is based on both microtubules and actin filaments (Kuznetsov et al., 1992; 1994). At present, several mechanisms have been proposed for the generation of forces that drive actin-dependent cellular activities, including forces arising from actin filament polymerization, and forces generated by motor proteins such as members of the myosin superfamily (Cramer et al., 1994).

The 43 kDa actin molecule (also known as globular, or G-actin) is a single polypeptide 375 amino acids long, and is associated with a molecule of ATP. Individual actin filaments consist of a helical arrangement of actin monomers, appearing in electron micrographs as strands approximately 8 nm wide (reviewed in Alberts et al., 1994). Myosin subfragment decoration of individual actin filaments

reveals the structural polarity of the actin filament, with the pointed end corresponding to the slow-growing (or "minus") end, and the barbed end corresponding to the fast-growing ("plus") end. In vitro, actin filaments engage in treadmilling: a process where net monomer addition at the barbed end is balanced by net loss from the pointed end, resulting in no net change in filament length.

The actin genes encode several structurally similar actin isoforms that mediate contractile function in muscle cells and motility in nonmuscle cells (Yao et al. 1995). Lower eukaryotes, such as yeasts, have a single essential actin gene (ACT1 in yeasts) (Welch et al. 1994). Higher eukaryotes express several different actin isoforms, each encoded by a separate gene (reviewed in Yao et al. 1995). These isoforms differ by <10% of their amino acid sequences. Despite the existence of multiple actin isoforms and their tissue-specific expression, their biological significance remains unknown. Structural comparisons may provide insights into the physiological significance of these isoforms (Rozycki et al., 1994).

Actin polymerization is a two step process (Southwick and Purich 1994). Several monomers bind together to form a short oligomer, forming a thermodynamically unstable nucleus. This is the rate-limiting, nucleation step. The second step involves the rapid addition of more monomers (reviewed in Pollard 1981). Two major factors influence the rate of filament elongation: the number of available nuclei, and the concentration of available actin monomers (Southwick and Purich 1994). Actin polymerization is also affected by the phosphorylation state of its adenine nucleotide (Pollard 1981). ATP-actin polymerizes much more rapidly

than ADP-actin, with a twenty-fold difference in their respective critical concentrations (Alberts et al. 1994). In vitro, there is a third step: the annealing of two filaments end-to-end, to form a longer filament (Pollard 1981). However, cells restrict the length of actin filaments *in vivo* through the action of various actin-binding proteins (Weeds et al., 1991; Fowler and Adam, 1992; Postner et al., 1992). After polymerization, the ATP bound to actin is rapidly hydrolyzed to ADP and P_i. Since the nucleotide on the filament does not exchange with that in the medium, actin monomers released during depolymerization probably contain bound ADP. Because ADP-actin has a lower affinity for filament ends, the monomers must exchange bound ADP for ATP before repolymerizing (Fecheimer and Zigmond, 1993).

As a rule, the reorganizations of microfilaments are driven by the assembly and disassembly of actin filaments, which in turn, are controlled by external signals (Stossel 1989). These include chemotactic stimuli, growth factors, and adhesion to the extracellular matrix (reviewed in Bershadsky et al. 1995). Instructions originating outside the cell ultimately control the formation and dissolution of actin filaments, either by directly affecting actin itself, and/or actin-binding proteins that regulate the polymerization- depolymerization events (Stossel 1993).

Actin-Binding Proteins

Actin binding proteins play a crucial role in mediating the structural and functional versatility of actin-based cellular events. These proteins control filament

assembly, adjust actin filament length, and define the three-dimensional organization of the actin cytoskeleton (Edwards et al., 1995). The multitude of actin binding proteins are classified according to how they modulate actin structure and function; thus, there are crosslinking proteins, actin filament-severing and nucleating proteins, capping proteins, and monomer-binding proteins (Hartwig and Kwiatkowski 1991, Weeds and Maciver 1993, Sun et al. 1995). This section will focus briefly on the major actin-binding proteins of each class.

In order to facilitate a rapid assembly of actin filaments in response to environmental stimuli, cells maintain a significant concentration of G-actin. This is accomplished through the expression of actin monomer binding proteins, as well as proteins that bind to the filament ends to prevent monomer addition (Hug et al. 1995). Thymosin β4 binds ATP-actin with high affinity in a 1:1 ratio, and is present in high concentrations within the cell (150-200 μM) (Southwick and Purich 1994). Vitamin D binding protein and DNAse I bind actin monomers 100-fold more tightly than thymosin β4, making monomeric actin less available for polymerization (Safer and Nachmias 1994).

Since the barbed ends of actin filaments compete with monomer-binding proteins, it is necessary for the barbed ends to be capped in order to prevent the nucleation of new filaments (Stossel 1989; 1993). Proteins that functionally cap filament ends, such as capping protein in *Dictyostelium*, are ubiquitous (Hug et al. 1995). One structurally related class of barbed end-capping proteins includes gelsolin, adseverin, and villin (Witke et al., 1992; 1995). This family of proteins

severs covalent bonds between actin subunits in a filament, and then remain firmly bound to the barbed ends of the fragmented filaments. The broken filaments can neither anneal nor elongate through the addition of actin monomers. The combined severing and capping functions of the gelsolin family may serve to break up existing actin filaments, enabling the monomers to be recycled to those cell regions actively forming new actin networks (Southwick and Purich 1994).

The actin crosslinking proteins have been isolated from a wide variety of cell types (Weeds and MacIver, 1991; Way et al., 1995). Actin filaments in vivo associate with actin crosslinking proteins to form three-dimensional arrays (Bershadsky and Vasiliev, 1989). Though highly diverse, this group of proteins shares the ability to bind at least two actin filaments (Hartwig and Kwiatkowski, 1991). These proteins organize actin filaments into isotropic networks or tightly linked bundles (Bershadsky and Vasiliev, 1989). Crosslinking proteins, such as filamin, spectrin, or actin-binding protein (ABP), tend to be high molecular weight, elongate molecules that form actin gels (Otto, 1994). In contrast, the actin bundling proteins are monomeric, globular molecules of much lower molecular weight than the so-called crosslinking proteins (Bershadsky and Vasiliev, 1989). Examples of bundling proteins include α-actinin, fimbrin, fascin, and *Dictyostelium* bundling protein. However, the distinction between these two classes of actin binding proteins is somewhat arbitrary, since there are crosslinking proteins that can perform the functions of bundling proteins, and vice versa (Otto, 1994).

The spectrin family is thought to play a role in maintaining the stability and

flexibility of many membrane skeletons (Hitt and Luna, 1994). Spectrin defects in human erythrocytes result in abnormalities in red cell shape, and can lead to hemolytic anemia. The elasticity of the erythrocyte membrane cytoskeleton has been partially attributed to changes in the extensibility of the spectrin rod domain and interactions between spectrin oligomers. Spectrin consists of an α and a β subunit, which may be bound together to form complex multimeric structures (Bershadsky and Vasiliev, 1989). In the erythrocyte, protein 4.1 and ankyrin are believed to link the spectrin-actin complex to integral plasma membrane proteins (Bretscher, 1993).

To summarize, it is the interactions between actin and its associated proteins that facilitates the multiplicity and plasticity of actin-dependent cellular processes. Over the past decade, a large number of actin-binding proteins have been isolated and classified according to their activities and locations (Weeds et al., 1991). Despite the significant advances in the identification and characterization of novel actin-binding proteins, several basic questions remain to be considered. How is the organization of microfilaments regulated in cells? What are the molecular mechanisms by which microfilaments associate with membranes? A number of model systems are currently being investigated in the hopes of answering these questions. These include the yeast, the slime mold *Dictyostelium*, cultured cell lines, the bacterial pathogen *Listeria*, and the fruitfly, *Drosophila*. Presently, the molecular interactions of the actin cytoskeleton with its regulatory proteins and the cell membrane remain unclear.

Actin Dynamics in the Drosophila Polytrophic Ovary: Functions of the *chickadee*, *quail*, and *singed* genes

The *Drosophila* ovary consists of several ovarioles, each of which contains numerous egg chambers arranged in an assembly-line fashion from early oogenesis to mature oocytes. At the anteriormost portion of each ovariole is the germarium, where the stem cell progenitor divides to generate a stem cell daughter and a cystoblast which will undergo four incomplete cytokinetic divisions to produce an egg chamber. The resulting 16 cells remain interconnected through cleavage furrows that develop into ring canals. Among the 16 cells, one develops into the oocyte while the remaining 15 become nurse cells.

Each of the *chickadee*, *singed*, and *quail* genes encode proteins homologous to known actin-binding proteins. The *chickadee* protein is homologous to profilin, an actin monomer-binding protein (Cooley et al., 1992). Recent work has shown that profilin regulates actin polymerization not by monomer sequestration, but by catalyzing the exchange between sequestered actin monomers and actin filaments (Sohn and Goldschmidt-Clermont 1994). In the presence of the actin-thymosin β4 complex, profilin promotes the rapid addition of actin monomers onto the barbed ends of filaments. The role of profilin in nurse cells may be to maintain the pool of actin monomers in the ATP-bound form by stimulating nucleotide exchange (Verheyen and Cooley, 1994). Since the actin filaments appear very rapidly, profilin may also be involved in mediating the

extracellular signal that triggers actin polymerization (Verheyen and Cooley, 1994).

The *chickadee* gene encodes two transcripts: one that is generally expressed, and the other specific to the germline (Verheyen and Cooley, 1994). Mutations disrupting either transcript result in various developmental defects. Null mutations of *chickadee* are lethal, indicating that profilin is essential in many ciritical developmental events. Mutations that disrupt the germline-specific transcript results in lack of the cytoplasmic actin filaments. However, the general *chickadee* transcript may also function in the germline. Mutations at the general *chickadee* locus results in disruption of germ cell cytokinesis. The regulation of mitosis is disrupted so that a random number of divisions occur, producing varying numbers of germline cells (Verheyen and Cooley, 1994).

In addition, profilin may also be required for the formation of cleavage furrows (Verheyen and Cooley, 1994). The failure of the final cytokinetic division in *chickadee* mutant egg chambers could be due to exhaustion of available profilin. Thus, although basal levels of profilin may be sufficient for some actin-dependent processes, higher concentrations are necessary for the formation of specialized cytoskeletal structures such as actin fibers and cytoplasmic bridges (Verheyen and Cooley, 1994). Further genetic analysis of profilin mutations is necessary in order to dissect the multiple profilin-dependent processes in *Drosophila* development.

The *singed* and *quail* genes are also involved in the formation of the cytoplasmic actin bundles. The phenotypes of both mutants are very similar to *chickadee* mutants, lacking the cytoplasmic actin bundles that should appear prior

to the rapid cytoplasmic transport phase. The *singed* protein is homologous to echinoderm fascin (Bryan et al., 1993). Fascin is present in the actin bundles of microvilli in sea urchin eggs and in the filopodial extensions of coelomocytes (Otto et al., 1980; Otto and Bryan, 1981). *Drosophila singed* protein is abundantly expressed in the nurse cell cytoplasm of wild-type egg chambers. Sterile *singed* mutants lack both the singed protein and the cytoplasmic actin bundles in nurse cells. The subcortical actin network remains unaffected. In addition, *singed* protein is required for the formation of the actin filament core in bristes (Cant et al., 1994; Tilney et al., 1995a).

Phenotypic and biochemical data strongly argue that singed is involved in actin bundling. *In vitro*, *singed* protein bundles actin filaments with the same stoichiometric and cross-banding pattern pattern as sea urchin fascin. *Drosophila singed* protein is expressed in the migratory cells of the egg chamber. The expression of *singed* in a wide variety of cell types in *Drosophila*, including the egg chamber, indicates its important conserved functions in the development and maintenance of actin bundles.

The *quail* gene encodes a villin-like protein. Unlike vertebrate villin, which is restricted to intestinal epithelial cells, the *Drosophila* villin-like protein is germline-specific. Early in oogenesis, the *quail* protein is located in the nurse cell subcortical actin networks. Just before the onset of rapid cytoplasmic transport, the *quail* protein colocalizes with the cytoplasmic actin bundles. Like singed, the *quail* protein could function to bundle cytoplasmic actin filament bundles into stable

arrays. Its subcortical distribution in the earlier stages of oogenesis suggests that quail may promote the nucleation of actin filaments at the region of cell membranes (Mahajan-Miklos and Cooley, 1994). Evidence so far indicates that the functions of the *singed* and *quail* proteins are not redundant. Both *singed* and *quail* function are probably required for different aspects of actin bundle assembly. Formation of a functional set of cytoplasmic actin bundles requires specific interactions between these (and possibly other) actin-binding proteins in the *Drosophila* egg chamber.

Ring Canals in the Drosophila Egg Chamber: Functions of the *kelch* and *hts* genes

Kelch mutants are defective in cytoplasmic transport from the nurse cells to the oocyte. Like hts, the *kelch* protein localizes specifically to ring canals. Unlike hts, kelch does not appear to be required for initial ring canal formation. However, in later stage *kelch* egg chambers, the actin and hts in the ring canals extend into the lumen of the cytoplasmic bridge, instead of forming a compact rim. This suggests that kelch interacts with actin and hts to form the highly organized inner rim (Xue and Cooley, 1993). The *kelch* protein was found to contain a BTB box and six kelch repeats. The function of the BTB box is unknown; however, the kelch BTB box can dimerize in solution. The kelch repeats are also found in a number of proteins, including the actin-binding scruin protein (Cooley and Therkauf, 1994). These observations suggest a model in which kelch dimerizes through its BTB box

to produce an actin binding molecule that cross-links and stabilizes actin filaments in the ring canals (Cooley and Therkauf, 1994).

Ring canal maturation involves the sequential addition of proteins as the egg chamber matures within the germarium (Robinson et al., 1994). At least one phosphotyrosine protein can be detected on the ring canals of newly-forming egg chambers in region 1 of the germarium. The role of phosphotyrosine protein(s) in the ring canal remains unknown. Hts and actin are present in region 2a, shortly after mitotic divisions are complete. Kelch is the last protein to be recruited to the ring canals, where it is first seen at region 3 of the germarium. Immunocytochemical studies reveal that at least one phosphotyrosine protein is associated with the membrane on the outer rim of the ring canal, and is distributed through the F-actin region. Hts and kelch are located in the inner rim, and are also present in the actin domain. In later stages, the ring canal rim is compacted, and all four of these proteins are co-localized. It is not clear whether more proteins are added to the ring canal as it matures from stage 3 to stage 10.

Studies on *Drosophila* mutants have provided valuable information on the molecular composition and development of ring canals. Additional proteins associated with cytokinetic furrows and ring canals have been identified, such as radixin (Sato et al., 1991), and CD43 (Yonemura et al., 1993). Further biochemical and molecular analysis of ring canals will provide information on their composition and function.

APPENDIX 2

Preliminary Results: Localization of Actin-Binding Proteins in the Rhodnius tropharium

One approach to understanding the mechanism and regulation of the actin mesh is to identify the proteins that are involved (Young et al., 1991; Margolis and Andreassen, 1993). I have attempted to determine if the chickadee, singed, hts, and kelch proteins are present in the *Rhodnius* ovariole using *Drosophila* monoclonal antibodies (a gift of Lynn Cooley, Yale University). However, immunofluorescence experiments using these antibodies failed to detect them in *Rhodnius*. Antibodies to phosphotyrosine, spectrin and myosin yielded promising results. These three antibodies stained the cortices of nurse cell lobes; and in the cases of spectrin and phosphotyrosine, a punctate staining pattern was also observed in the nurse cell cytoplasm. None of the antibodies used stained the actin mesh in the trophic core.

Materials and Methods

All steps were performed at room temperature unless stated otherwise. Ovarioles were removed and desheathed in Ringers solution. Some ovarioles were first incubated in 0.1% elastase in MF buffer for 3-5 mins. They were then permeabilized in 0.1% Triton X-100 in MF buffer, pH 7.1-7.3, for approximately 10 mins. The tissue was fixed for 30 mins - 1 hour in 2-5% paraformaldehyde in MF buffer, at 4°C, and then washed in several changes of MF buffer or PBS containing

0.1% Triton X-100 over a period of 30 mins. To minimize nonspecific binding, the ovarioles were blocked in 1 - 3% bovine serum albumin (BSA) in MF buffer for 1 hour. Incubation in the 1° antibody for 1 - 1.5 hours at 37°C was followed by several washes in 1 - 3% BSA in MF buffer or PBS with 0.1% Triton X-100 over a 45 min. period. The ovarioles were then incubated in the appropriate 2° antibody for 1 - 1.5 hours in the dark, and washed in PBS for a minimum of 30 mins. The tissue was mounted in PBS mixed with 1-5 mg/ml n-propyl gallate as an anti-fadant. Photomicrographs were taken using a Zeiss Photo II microscope on T-Max 400 film. The film was developed in T-Max developer according to manufacturer's instructions. Controls were incubated in 2° antibody alone.

The 1° antibodies used in these experiments were the chickadee, singed, kelch, and hts proteins (a generous gift of Lynn Cooley, Yale University). These antibodies were mouse hybridoma cell line monoclonal antibodies to the *Drosophila* proteins. The antibodies to *chickadee* and *singed* were used undiluted, and those for *kelch* and *hts* were diluted 1:1 in PBS with 0.3% Triton-X 100 and 0.5% bovine serum albumin.

Primary antibodies for spectrin (Sigma S-1390), phosphotyrosine (Upstate Biotechnology Inc. 05-321), and myosin (Sigma M-7648) were obtained commercially. Dilutions for the commercial antibodies were 1:40, 1:100, and 1:40, respectively, in PBS with 0.1% bovine serum albumin.

Preliminary Results

Spectrin is localized in the germ cell lobes in the 5th instar, as well as the

nurse cell cortices in the adult (Plate I). A punctate staining pattern is also present in some of the nurse cells in the adult tropharium (Figs. A, C). Myosin appears to be localized in the nurse cell cortices and cytoplasm in the adult (Figs. E, F). The nucleus is devoid of myosin.

Anti-phosphotyrosine antibodies stain the nurse cell cortices and cytoplasm in the adult, as well as the cortices of germ cells in the 5th instar (Plate II). A punctate staining pattern was observed in the sheath cells (Fig. J). The inner sheath cells and the cortices of the follicle cells surrounding the oocyte label strongly (Figs. K, M).

In all of the immunofluorescence experiments, control preparations were incubated in only the secondary antibody, without prior incubation in the primary antibody. Instead of incubation in the primary antibody, the control preparations were incubated in 1% bovine serum albumin in PBS. All of the control preparations exhibited negligible amounts of fluorescence, and are therefore not depicted in the preliminary results.

Plate I

Spectrin and myosin localization in 5th instar and adult ovarioles

Figs A-D depict ovarioles stained with a rabbit antibody to chicken spectrin, visualized with FITC-conjugated goat anti-rabbit antibody.

Fig. A.
This fluorescence micrograph depicts the pattern of spectrin staining in an adult tropharium. There is distinct labelling of the nurse cell cortices, as well as a punctate staining pattern in the cytoplasm.
1,250X

Fig. B.
The germ cell cortices in this 7 dpf ovariole are labelled with the anti-phosphotyrosine antibody.
2,000X

Fig. C.
Higher magnification of the punctate staining pattern in the nurse cells of the adult tropharium.
3,250X

Fig. D.
There is uneven staining in the sheath cells of this 13 dpf germarium. Some of the cells appear to stain more intensely than others.
2,500X

Figs. E & F.
Both figures illustrate the pattern of myosin staining in the nurse cell lobes of an adult ovariole. Here, FITC-labelled goat anti-rabbit antibody was used to visualize the myosin labelling. The nurse cell cortices and cytoplasm exhibit some labelling. Control preparations displayed negligible amounts of fluorescence in comparison.
3,500X; 3,500X

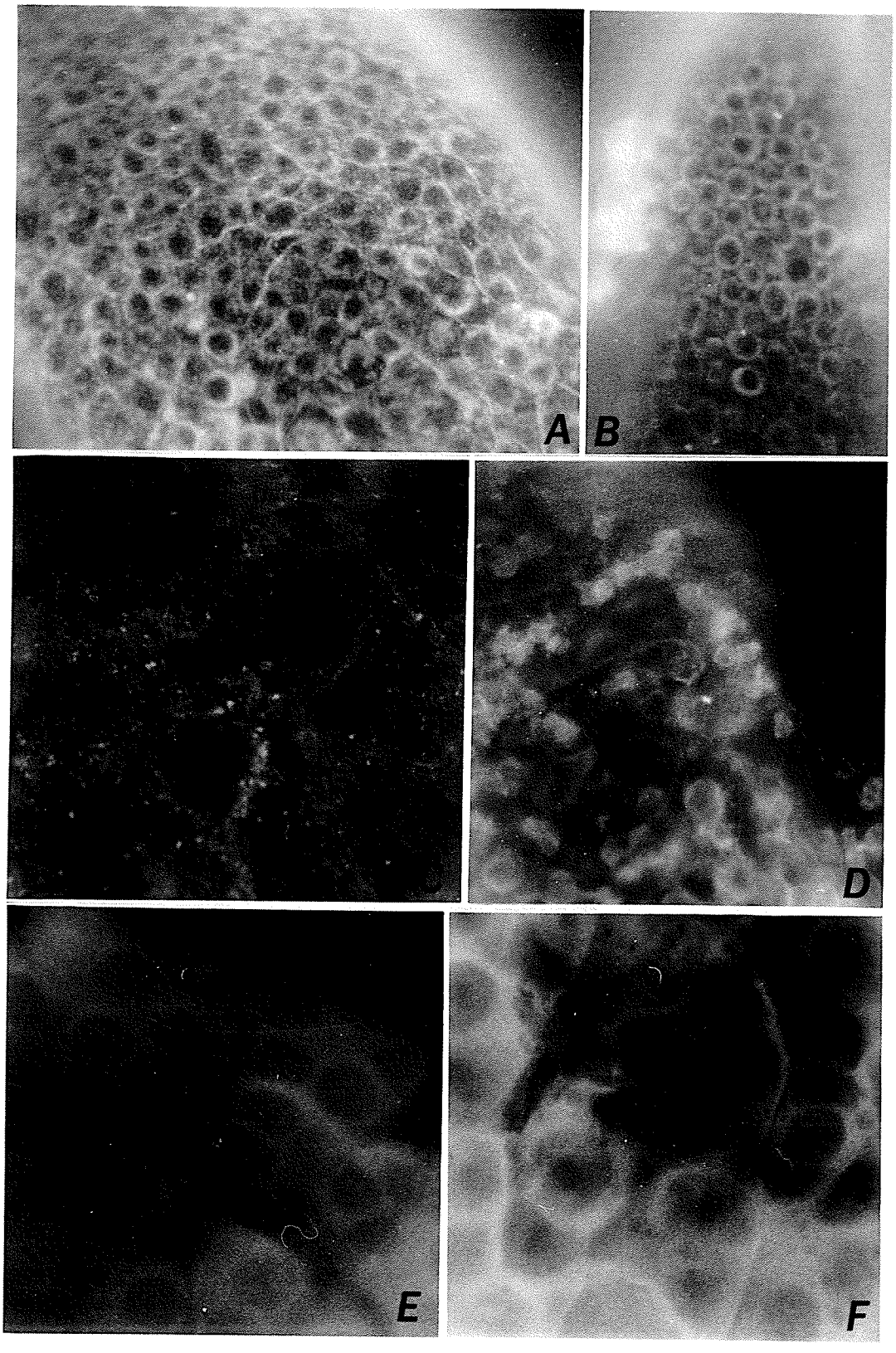
A
B
D
E
F

Plate II

Phosphotyrosine localization.

This plate illustrates phosphotyrosine staining in the ovarioles of 5th instar and adult *Rhodnius*.

Fig. G.
The nurse cell cortices are labelled. This micrograph illustrates the pattern of phosphotyrosine staining towards the posterior region of the tropharium. Clusters of nurse cell nuclei are visible (black arrows). The nuclei are not labelled (white arrows).
3,500X

Fig. H.
This *Drosophila* control preparation demonstrates that the phosphotyrosine antibody is localized to the ring canals in the egg chambers.
2,500X

Fig I.
The germ cell cortices in this 7 dpf ovariole are labelled with the phosphotyrosine antibody.
938X

Fig. J.
A punctate staining pattern is visible in the germ cells in the 14 dpf germarium.
2,000X

Fig. K.
The inner sheath cells are strongly labelled in this preparation.
2,200X

Figs. L & M.
These micrographs depict the staining pattern in the follicle cells. Fig. L. depicts a strand of follicle cells that was separated from the oocyte. Fig. M. shows the staining pattern in the cortices of the follicle cells that envelop the oocytes.
1,500X; 1,000X

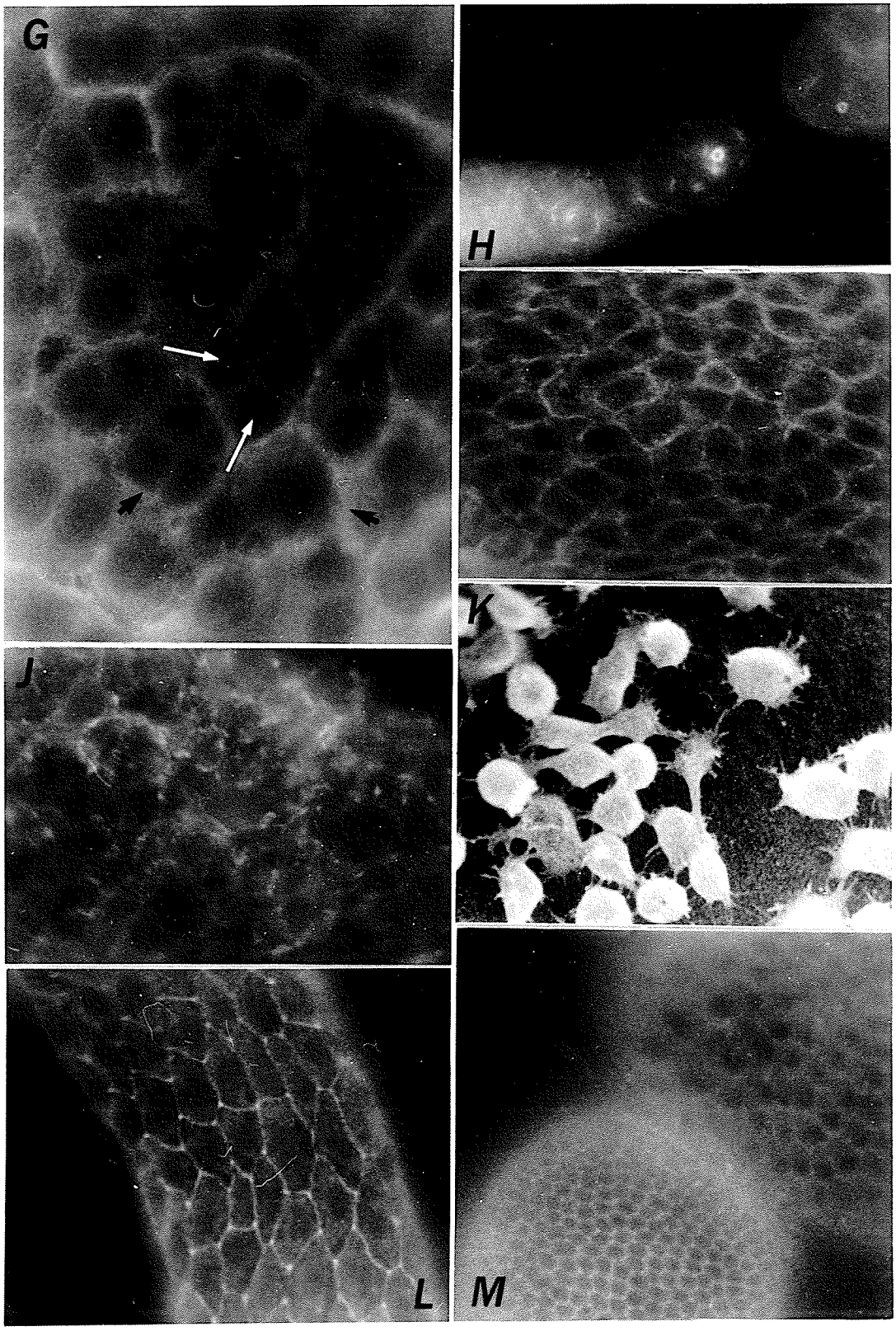
G
H
K
J
L
M

LITERATURE CITED

Alberts, B., D. Bray, J. Lewis, M. Raff, K. Roberts and J. D. Watson. 1994. Molecular Biology of the Cell. New York, Garland Publishing.

Anderson, E., and E. Huebner. 1968. Development of the oocyte and its accessory cells of the polychaete, *Diopatra cuprea*. Journal of Morphology 126: 163-98.

Barkalow, K. and J. H. Hartwig. 1995. The role of actin filament barbed-end exposure in cytoskeletal dynamics and cell motility. Biochemical Society Transactions 23: 451-59.

Bearer, E. L., J. A. DeGiorgis, R. A. Bodner, A. W. Kao and T. S. Reese. 1993. Evidence for myosin motors on organelles in squid axoplasm. Proceedings of the National Academy of Sciences of the U.S.A. 90: 11252-56.

Bershadsky, A. D., U. Gluck, O. N. Denisenko, T. V. Sklyarova, I. Spector and A. Ben-Ze'ev. 1995. The state of actin assembly regulates actin and vinculin expression by a feedback loop. Journal of Cell Science 108: 1183-93.

Bershadsky, A.D., and J.M. Vasiliev. 1989. Cytoskeleton. Plenum Press:New York. p. 13-73.

Bohrmann, J., and K. Biber. 1994. Cytoskeleton-dependent transport of cytoplasmic particles in previtellogenic to midvitellogenic ovarian follicles of *Drosophila*: Time-lapse analysis using video-enhanced contrast microscopy. Journal of Cell Science 107: 849-58.

Bray, D., and J.G. White. 1988. Cortical flow in animal cells. Science 236:1086-91.

Bretscher, A. 1993. Microfilaments and membranes. Current Opinion in Cell Biology 5:653-660.

Bryan, J., R. Edwards, P. Matsudaira, J. Otto and J. Wulfkuhle. 1993. Fascin, an echinoid actin-bundling protein, is a homolog of the Drosophila singed gene product. Proceedings of the National Academy of Sciences of the U.S.A. 90: 9115-19.

Cant, K., B. A. Knowles, M. S. Mooseker and L. Cooley. 1994. Drosophila Singed, a fascin homolog, is required for actin bundle formation during oogenesis and bristle extension. Journal of Cell Biology 125(2): 369-380.

Cao, L.-G. and Y.-L. Wang. 1990. Mechanism of the formation of contractile ring in dividing cultured animal cells. I. Recruitment of preexisting actin filaments into

the cleavage furrow. Journal of Cell Biology 110: 1089-1095.

Cao, L.-G., D. J. Fishkind and Y.-L. Wang. 1993. Localization and dynamics of nonfilamentous actin in cul;tured cells. Journal of Cell Biology 123(1): 173-181.

Chia , C.P., A. Shariff, S.A. Savage, and E.J. Luna. 1993. The intergral membrane protein, ponticulin, acts as a monomer in nucleatin actin assembly. Journal of Cell Biology 120: 909-22.

Cooley, L., E. Verheyen and K. Ayers. 1992. Chickadee encodes a profilin required for intercellular cytoplasm transport during Drosophila oogenesis. Cell 69: 173-184.

Cooley, L. and W. E. Therkauf. 1994. Cytoskeletal functions during Drosophila oogenesis. Science 266(28): 590-595.

Cramer, L. P., T. J. Mitchison and J. A. Theriot. 1994. Actin-dependent motile forces and cell motility. Current Opinion in Cell Biology 6: 82-86.

Edwards, R. A., H. Herrera-Sosa, J. Otto and J. Bryan. 1995. Cloning and expression of a murine fascin homolog from mouse brain. Journal of Biological Chemistry 270: 10764-70.

Faulstich, H., S. Zobeley, D. Heintz., and G. Drewes. 1993. Probing the phalloidin binding site of actin. FEBS Letters 318: 218-22.

Fechheimer, M. and S. H. Zigmond. 1993. Focusing on unpolymerized actin. Journal of Cell Biology 123(1): 1-5.

Field, C. M. and B. M. Alberts. 1995. Anillin, a contractile ring protein that cycles from the nucleus to the cell cortex. Journal of Cell Biology 131: 165-178.

Fowler, V. M. and E. J. H. Adam. 1992. Spectrin redistributes to the cytosol and is phosphorylated during mitosis in cultured cells. Journal of Cell Biology 119(6): 1559-1572.

Goslin, K., E. Birgbauer, G. Banker and F. Solomon. 1989. The role of cytoskeleton in organizing growth cones: a microfilament-associated growth cone component depends upon microtubules for its localization. Journal of Cell Biology 109: 1621-31.

Gottlieb, E. 1990. Messenger RNA transport and localization. Current Opinion in Cell Biology 2: 1080-1086.

Gutzeit, H. O. and R. Koppa. 1982. Time-lapse film analysis of cytoplasmic

streaming during late oogenesis of Drosophila. Journal of Embryology and Experimental Morphology 67: 101-111.

Gutzeit, H. O. 1986. The role of microfilaments in cytoplasmic streaming in Drosophila follicles. Journal of Cell Science 80: 159-169.

Gutzeit, H. O. and E. Huebner. 1986. Comparison of microfilament patterns in nurse cells of different insects with polytrophic and telotrophic ovarioles. Journal of Embryology and Experimental Morphology 93: 291-301.

Harrison, R., and E. Huebner, 1994. Immunocytochemistry and polarity of the microtubule arrays in the telotrophic ovary of the insect *Rhodnius prolixus*. Molecular Biology of the Cell 5(suppl.): 262a, abstract 1636.

Hartwig, J. H. and D. J. Kwiatkowski. 1991. Actin-binding proteins. Current Opinion in Cell Biology 3: 87-97.

Hitt, A.L., and E.J. Luna. 1994. Membrane interactions with the actin cytoskeleton. Current Opinion in Cell Biology 6:120-30.

Huebner, E. 1982. Ultrastructure and development of the telotrophic ovary. In H. Akai, R.C. King and S. Morohoshi (eds.). The Ultrastructure and Functioning of Insect Cells. Tokyo,Japan: Society for Insect Cells Japan.

Huebner, E. 1984. The ultrastructure and development of the telotrophic ovary. In R.C. King and Akai (ed.). Insect Ultrastructure Vol. 2. New York: Plenum Press. p. 3-48.

Huebner, E., and E. Anderson. 1972. A cytological study of the ovary of *Rhodnius prolixus*. III. Cytoarchitecture and development of the trophic chamber. Journal of Morphology 138:1-40.

Huebner, E. and H. O. Gutzeit. 1986. Nurse cell-oocyte interaction: A new F-actin mesh associated with the microtubule-rich core of an insect telotrophic ovariole. Tissue and Cell 18(5): 753-764.

Huebner, E., K. Yeow., and D. Lococo. 1993. A unique nurse cell-oocyte model: germ cells of the polychaete, *Ophryotrocha labronica*. Molecular Biology of the Cell 4 (suppl.):134.

Hug, C., P. Y. Jay, I. Reddy, J. G. McNally, P. C. Bridgman, E. L. Elson and J. A. Cooper. 1995. Capping protein levels influence actin assembly and cell motility in Dictyostelium. Cell 81: 591-600.

Johnston, D.St. and C. Nusslein-Volhard. 1992. The origin of pattern and polarity in the Drosophila embryo. Cell 68: 201-219.

Kelly, G.M. 1989. Embryogenesis of the insect, *Rhodnius prolixus*: Cellular, biochemical, and molecular aspects. PhD Thesis, University of Manitoba.

King, R.C., J.D. Cassidy, and A. Rousset. 1982. The formation of clones of interconnected cells during gametogenesis in insects. In R.C. King and H. Akai (eds.) Insect Ultrastructure Vol. I. New York: Plenum Press: p. 3-31.

King, R.C., and P.D. Storto. 1988. The role of the *otu* gene in *Drosophila* oogenesis. Bioessays 8:18-24.

Koch, E.A., and R.C. King. 1966. The origin and early differentiation of the egg chamber of *Drosophila melanogaster*. Z. Zellforsch. 102: 129-52.

Kuznetsov, S., G. M. Langford and D. G. Weiss. 1992. Actin-dependent organelle movement in squid axoplasm. Nature 356(722-25).

Kuznetsov, S., D. T. Riviera, F. F. Severin, D. G. Weiss and G. M. Langford. 1994. Movement of axoplasmic organelles on actin filaments from skeletal muscle. Cell Motility and Cytoskeleton 28: 231-42.

Langford, G. M. 1995. Actin- and microtubule-dependent organelle motors: interrelationships between the two motility systems. Current Opinion in Cell Biology 7: 82-8.

Lasko, P. F. 1992. Molecular movements in oocyte patterning and pole cell differentiation. BioEssays 14(8): 507-512.

Lin, C.-H. and P. Forscher. 1993. Cytoskeletal remodeling during growth cone-target interactions. Journal of Cell Biology 121: 1369-83.

Lin, H., L. Yue and A. Spradling. 1994. The Drosophila fusome, a germline-specific organelle, contains membrane skeletal proteins and functions in cyst formation. Development 120: 947-956.

Lutz, D.A. 1979. Structural and physiological aspects of 5th instar ovarian development in *Rhodnius prolixus*. M.Sc. Thesis, University of Manitoba.

Lutz, D., and E. Huebner. 1980. Development and cellular differentiation of an insect telotrophic ovary (*Rhodnius prolixus*). Tissue and Cell 12: 773-94.

Lutz, D. A. and E. Huebner. 1981. Development of nurse cell-oocyte interactions

in the insect telotrophic ovary (Rhodnius prolixus). Tissue and Cell 13(2): 321-335.

Mahajan-Miklos, S. and L. Cooley. 1994. The villin-like protein encoded by the Drosophila quail gene is required for actin bundle assembly during oogenesis. Cell 78: 291-301.

Margolis, R. L. and P. R. Andreassen. 1993. The telophase disc: its possible role in mammalian cell cleavage. BioEssays 15: 201-7.

McPherson, S. M. G. and E. Huebner. 1993. Dynamics of the oocyte cortical cytoskeleton during oogenesis in Rhodnius prolixus. Tissue and Cell 25(3): 399-421.

O'Donnell, M.J. 1985. Calcium action potentials in the developing oocytes of an insect, *Rhodnius prolixus.* Journal of Experimental Biology 119:287-300.

Otto, J. J., R. E. Kane and J. Bryan. 1980. Redistribution of actin and fascin in sea urchin eggs after fertilization. Cell Motility 1: 31-40.

Otto, J. J. and J. Bryan. 1981. The incorporation of actin and fascin into the cytoskeleton of filopodial sea urchin coelomocytes. Cell Motility 1: 179-92.

Otto, J. J. 1994. Actin-bundling proteins. Current Opinion in Cell Biology 6: 105-9.

Pollard, T. D. 1981. Cytoplasmic contractile proteins. Journal of Cell Biology 91: 156s-165s.

Postner, M. A., K. G. Miller and E. F. Wieschaus. 1992. Maternal effect mutations of the sponge locus affect actin cytoskeletal rearrangements in Drosophila melanogaster embryos. Journal of Cell Biology 119: 1205-1218.

Robinson, D. N., K. Cant and L. Cooley. 1994. Morphogenesis of Drosophila ovarian ring canals. Development 120: 2015-2025.

Rozycki, M., J. C. Myslik, C. E. Schutt and U. Lindberg. 1994. Structural aspects of actin-binding proteins. Current Opinion in Cell Biology 6: 87-95.

Safer, D. and V. T. Nachmias. 1994. Beta thymosins as actin-binding peptides. BioEssays 16(7): 473-79.

Sato, N., S. Yonemura, T. Obinata, S. Tsukita and S. Tsukita. 1991. Radixin, a barbed end-capping actin-modulating protein, is concentrated at the cleavage furrow during cytokinesis. Journal of Cell Biology 113(2): 321-330.

Satterwhite, L. L. and T. D. Pollard. 1992. Cytokinesis. Current Opinion in Cell Biology 4: 43-52.

Shariff, A., and E.J. Luna. 1990. *Dictyostelium discoideum* plasma membranes contain an actin-nucleating activity that requires ponticulin, an integral membrane glycoprotein. Journal of Cell Biology 110:681-92.

Sohn, R. H. and P. J. Goldschmidt-Clermont. 1994. Profilin: at the crossroads of signal transduction and the actin cytoskeleton. BioEssays 16(7): 465-72.

Southwick, F. S. and D. L. Purich. 1994. Dynamic remodelling of the actin cytoskeleton: lessons learned from Listeria locomotion. BioEssays 16: 885-91.

Spradling, A. 1993. Germline cysts: Communes that work. Cell 72: 649-51.

Stossel, T. P. 1989. From signal to pseudopod. Journal of Biological Chemistry 264: 18261-64.

Stossel, T. P. 1993. On the crawling of animal cells. Science 260: 1086-93.

Sun, H.-Q., K. Kwiatkowsky and H. L. Yin. 1995. Actin monomer binding proteins. Current Opinion in Cell Biology 7: 102-110.

Symons, M.H., and T.J. Mitchison. 1991. Control of actin polymerization in live and permeabilized fibroblasts. Journal of Cell Biology 114: 503-13.

Therkauf, W. E., S. Smiley, M. L. Wong and B. M. Alberts. 1992. Reorganization of the cytoskeleton during Drosophila oogenesis: implications for axis specification and intercellular transport. Development 115: 923-936.

Tilney, L. G., M. S. Tilney and G. M. Guild. 1995a. F-actin bundles in Drosophila bristles I: two filament cross-links are involved in bundling. Journal of Cell Biology 130(3): 629-638.

Tilney, L.G., M.S. Tilney, and G.M. Guild. 1995b. Formation of actin filament bundles in the ring canals of developing *Drosophila* follicles. Molecular Biology of the Cell 6 (suppl.):825.

Tranter, M. P., S. P. Sugrue and M. A. Schwartz. 1991. Binding of actin to liver cell membranes: the state of membrane-bound actin. Journal of Cell Biology 112(5): 891-901.

Valdimarsson, G. and E. Huebner. 1989. The developemnt of microtubular arrays in the germ tissue of an insect telotrophic ovary. Tissue and Cell 21(1): 123-138.

Venable, J.M., and R. Coggeshall. 1965. A simplified lead citrate stain for use in electron microscopy. Journal of Cell Biology 25: 407-12.

Verheyen, E. M. and L. Cooley. 1994. Profilin mutations disrupt multiple actin-dependent processes during Drosophila development. Development 120: 717-728.

Warn, R. M., H. O. Gutzeit, L. Smith and A. Warn. 1985. F-actin rings are associated with the ring canals of the Drosophila egg chamber. Experimental Cell Research 157: 355-363.

Way, M., M. Sanders, M. Chafel, Y.-H. Tu, A. Knight and P. Matsudaira. 1995. B-scruin, a homologue of the actin crosslinking protein scruin, is localized to the acrosomal vesicle of Limulus sperm. Journal of Cell Science 108: 3155-62.

Weeds, A. G., J. Gooch, M. Hawkins, B. Pope and M. Way. 1991. Role of actin-binding proteins in cytoskeletal dynamics. Biochemical Society Transactions 19: 1016-20.

Weeds, A. and S. Maciver. 1993. F-actin capping proteins. Current Opinion in Cell Biology 5: 63-69.

Welch, M.D., D.A. Holtzmann, and D.G. Drubin. 1994. The yeast actin cytoskeleton. Current Opinion in Cell Biology 6:110-19.

Witke, W., M. Schleicher and A. A. Noegel. 1992. Redundancy in the microfilament system: abnormal development of Dictyostelium cells lacking two F-actin cross-linking proteins. Cell 68: 53-62.

Witke, W., A. H. Sharpe, J. H. Hartwig, T. Azuma, T. P. Stossel and D. J. Kwiatkowski. 1995. Hemostatic, inflammatory, and fibroblast responses are blunted in mice lacking gelsolin. Cell 81: 41-51.

Xue, F. and L. Cooley. 1993. *kelch* encodes a component of intercellular bridges in Drosophila egg chambers. Cell 72: 681-693.

Yao, X., C. Chaponnier, G. Gabbiani and J. G. Forte. 1995. Polarized distribution of actin isoforms in gastric parietal cells. Molecular Biology of the Cell 6: 541-57.

Yonemura, S., A. Nagafuchi, N. Sato and S. Tsukita. 1993. Concentration of an intergral membrane protein, CD43 (leukosialin, sialophorin), in the cleavage furrow through the intercation of its cytoplasmic domain with actin-based cytoskeletons. Journal of Cell Biology 120: 437-49.

Young, P. E., T. C. Pesacreta and D. P. Kiehart. 1991. Dynamic changes in the distribution of cytoplasmic myosin during Drosophila embryogenesis. Development 111: 1-14.

Yue, L. and A. Spradling. 1992. *Hu-li tai shao*, a gene required for ring canal formation during Drosophila oogenesis, encodes a homolog of adducin. Genes and Development 6: 2443-2454.

Zamboni, L., and B. Gondos. 1968. Intercellular bridges and syncronization of germ cell differentiation during oogenesis in the rabbit. Journal of Cell Biology 36:276-82.